https://doi.org/10.5194/egusphere-2026-3460
Preprint. Discussion started: 5 August 2026

Monsoon-influenced terrestrial forcing shapes inter-reef carbonate production (Spermonde Archipelago, Indonesia)

Marleen Stuhr[1†], Yannis Kappelmann[1,2†], Thomas Mann[1,3], Dominik Kneer[1], Jamaluddin Jompa[4], Hildegard Westphal[1,2]

† Shared first authors
[1]Leibniz Centre for Tropical Marine Research (ZMT), 28359 Bremen, Germany
[2]University of Bremen, 28359 Bremen, Germany
[3]Federal Institute for Geosciences and Natural Resources (BGR), 30655 Hannover, Germany
[4]Hasanuddin University (UNHAS), Makassar, South Sulawesi 90245, Indonesia

Correspondence to: Marleen Stuhr (marleen.stuhr@leibniz-zmt.de)

Abstract. Monsoon-driven fluvial discharge exerts strong environmental control on water quality and carbonate sediment composition in tropical shelf systems, yet the capacity of photosymbiont-bearing calcifiers to sustain carbonate production under monsoon-amplified turbidity and nutrient loading across semi-enclosed platforms remains poorly understood. We here investigate inter-reef facies patterns and benthic foraminiferal assemblages across the Spermonde Archipelago (southwest Sulawesi, Indonesia), a land-attached tropical carbonate shelf subject to seasonal monsoon runoff and intensifying coastal development, using geochemical, sedimentological, and foraminiferal analyses of 51 inter-reef seafloor samples. Nearshore sediments are enriched in mud and organic matter, and dominated by heterozoan and stress-tolerant assemblages, yielding low values for the FoRAM Index (FI; an index that increases with the relative abundance of photosymbiont-bearing foraminifera), indicating conditions unfavourable for photosymbiont-bearing carbonate producers. Statistical separation of nearshore facies from all mid- and outer-shelf assemblages supports a threshold rather than gradual cross-shelf transition. This threshold is spatially asymmetrical, extending further offshore in the northern sector, likely reflecting enhanced retention of fluvially derived material within the more enclosed northern shelf geometry, with the southward Makassar Strait circulation limiting offshore dispersal. Mid- and outer-shelf deposits (~80% of the investigated area) are characterised by foramol facies dominated by benthic foraminifers, bivalves and gastropods, with *Amphistegina* and *Operculina* as the dominant symbiont-bearing foraminifera; FI values increase progressively offshore, reflecting improving photic conditions as terrestrially driven seasonal turbidity decreases with distance from the coast. Strong spatial correspondence between foraminiferal assemblages and independently derived sedimentary facies, including convergence of the foraminiferal community transition zone with foramol mud-supported carbonate sediment facies, validates the FI as an ecological proxy beyond shallow reef settings and demonstrates its utility in differentiating carbonate production modes in mesotrophic equatorial systems. These findings support a carbonate production continuum in which photozoan and heterozoan components are organised non-linearly along environmental gradients, with threshold responses emerging from the interaction of platform geometry and catchment-scale terrestrial forcing under seasonal monsoon modulation. We therefore interpret the Spermonde shelf as spatially structured by shifting autotrophic-heterotrophic balances, rather than discrete facies categories.

https://doi.org/10.5194/egusphere-2026-3460
Preprint. Discussion started: 5 August 2026

1 Introduction

Coastal Southeast Asia is characterized by some of the highest nutrient concentrations persistent in tropical marine environments, resulting from the interaction of seasonal monsoon-driven precipitation and resulting fluvial discharge, in addition to episodic upwelling, superimposed on increasingly intensive land use in densely populated hinterlands and urbanized coastlines (Morgan et al., 2020; Rankey et al., 2023; Yasir Haya and Fujii, 2017). At the same time, these waters also host the core of the Coral Triangle, the global hotspot of coral and reef biodiversity (Förderer et al., 2018; Veron et al., 2009). This juxtaposition of elevated nutrient supply and high diversity challenges classical distinctions between oligotrophic, photozoan-dominated carbonate systems and nutrient-rich, heterozoan-dominated shelves (Carannante et al., 1988; James, 1997; Lees and Buller, 1972). Tropical coastal systems are increasingly understood to operate along a continuum of carbonate production modes, in which photozoan and heterozoan components coexist and vary in response to environmental gradients such as nutrient availability, light penetration and hydrodynamic setting (Brandano et al., 2022; Westphal et al., 2010; Wilson and Vecsei, 2005). Within such continua, however, responses are not necessarily linear as semi-enclosed platforms subject to strong terrestrial forcing may exhibit pronounced threshold-like shifts at specific points along the gradient, where relatively small changes in nutrient or sediment input translate into disproportionate ecological responses. This calls for integrative approaches that link ecological processes to sedimentary products.

Analyses of skeletal carbonate assemblages provide a powerful means to bridge ecology and sedimentology, allowing both the reconstruction of environmental conditions in the geological record and the assessment of modern carbonate systems operating under anthropogenic pressure (e.g., Brandano et al., 2022; Wright and Burgess, 2005). In particular, benthic foraminifera respond sensitively to variations in nutrient availability, substrate type, and photic conditions, while simultaneously acting as major carbonate sediment producers in many tropical and subtropical settings (Hallock et al., 2003; Narayan et al., 2022). Functional differentiation into symbiont-bearing, heterotrophic, and stress-tolerant taxa provides a framework to interpret environmental gradients in terms of light availability and nutrient load. The FoRAM Index (FI; Hallock, 2012; Hallock et al., 2003) integrates these functional groups into a quantitative proxy for environmental suitability/conditions and has been widely applied in shallow tropical Indo-Pacific reef environments, including coastal areas adjacent to major urban centres and within marine protected areas (e.g., Gonzales et al., 2022; Natsir, 2022). On the Spermonde shelf specifically, large benthic foraminifera (LBF) distributions in reef environments have previously been shown to respond sensitively to gradients in light availability, hydrodynamic energy and nutrient supply (Girard et al., 2025; Renema, 2018; Renema et al., 2001), suggesting that foraminiferal assemblages may record cross-shelf environmental gradients beyond the shallow reef settings for which the FI was originally developed. However, its performance across deeper inter-reef shelf settings influenced by monsoon-driven terrestrial input remains less explored.

The Spermonde Archipelago, located near the southwestern corner of the Coral Triangle offshore SW Sulawesi, Indonesia, represents a natural laboratory for studying the interaction between fluvial input, monsoon seasonality, reef-derived carbonate production, and human modification of coastal systems. Strong nearshore–offshore gradients in water quality, benthic community structure and ecosystem functioning have been documented across the shelf, reflecting the combined influence of coastal development and hydrodynamic forcing (e.g., Estradivari et al., 2025; Girard et al., 2022, 2025). These resulting turbidity gradients are not only affecting coral and algal assemblages, but also the distribution of reef-associated LBF communities (Girard et al., 2025; Renema, 2018; Renema et al., 2001; Renema and Troelstra, 2001). Reviews of equatorial carbonate systems emphasize that

https://doi.org/10.5194/egusphere-2026-3460
Preprint. Discussion started: 5 August 2026

tropical shelves influenced by high rainfall and runoff commonly deviate from classical oligotrophic reef models, instead forming mixed or oligophotic systems characterized by reduced light penetration and elevated nutrient availability, yet LBF remain widely present and continue to contribute substantially to carbonate production (Wilson, 2002, 2012). Therefore, carbonate production is best understood as a continuum of mixed photozoan-heterozoan modes (James, 1997) structured by environmental gradients, rather than as binary opposition between discrete end-member systems (Wilson and Vecsei, 2005; Wright and Burgess, 2005). Despite substantial progress in the understanding of the carbonate facies continuum, little research still been done on the composition and distribution of deeper inter-reef sediments, the ecological signals recorded within them, and their role within the carbonate budget. Moreover, the extent to which benthic foraminiferal assemblages and derived FI values capture spatial threshold responses to terrestrial nutrient input across the shelf systems has not been systematically evaluated.

This study integrates sedimentological, geochemical, and benthic foraminiferal data from 51 seafloor samples taken across the Spermonde shelf to (a) characterize spatial facies patterns in inter-reef setting, (b) evaluate how benthic foraminiferal functional groups vary along the nearshore-offshore gradient, (c) assess the FI as a relative proxy for environmental gradients beyond shallow reef environments, and (d) identify threshold responses and spatial asymmetries that inform broader models of carbonate system organization in nutrient-influenced tropical settings.

1.1 Study area

The Spermonde Archipelago is located between 4.5°S to 5.3°S and 119°E to 119.5°E offshore SW Sulawesi, Indonesia (Fig. 1A, B). It comprises numerous shallow-water coral reefs distributed across a gently inclined (<1°) carbonate platform (Fig. 1C) that extends between ~35 km in the south and up to ~70 km in the central shelf from the mainland to the Strait of Makassar (Renema and Troelstra, 2001). The semi-enclosed shelf system is bordered by a discontinuous reef rim along its western margin that restricts exchange with the open Makassar Strait.

The shelf has been subdivided into nearshore, mid-shelf, and outer-shelf zones, based on bathymetry and coral reef distribution (Renema et al., 2001). This zonation has been adopted in recent sedimentological, geomorphological and ecological studies of the archipelago (e.g., Estradivari et al., 2025; Janßen et al., 2017; Kench and Mann, 2017; Sengupta et al., 2025; Teichberg et al., 2018). The framework was originally defined for the central shelf sector but is applied here across the full north–south extent of the archipelago to roughly structure the spatial framework of the study (Fig 1C). The nearshore zone reaches water depths of ~20 m in the central and northern shelf and ~30 m in the south, and is characterized by small patch reefs rising from shallow water. The mid-shelf (~20-40 m depth) hosts numerous larger reef complexes. Toward the outer shelf, a 5 to 10 km wide trough with water depths of 50 to more than 60 m and scarce reef growth separates the mid-shelf reefs from the outer rim system.

https://doi.org/10.5194/egusphere-2026-3460
Preprint. Discussion started: 5 August 2026

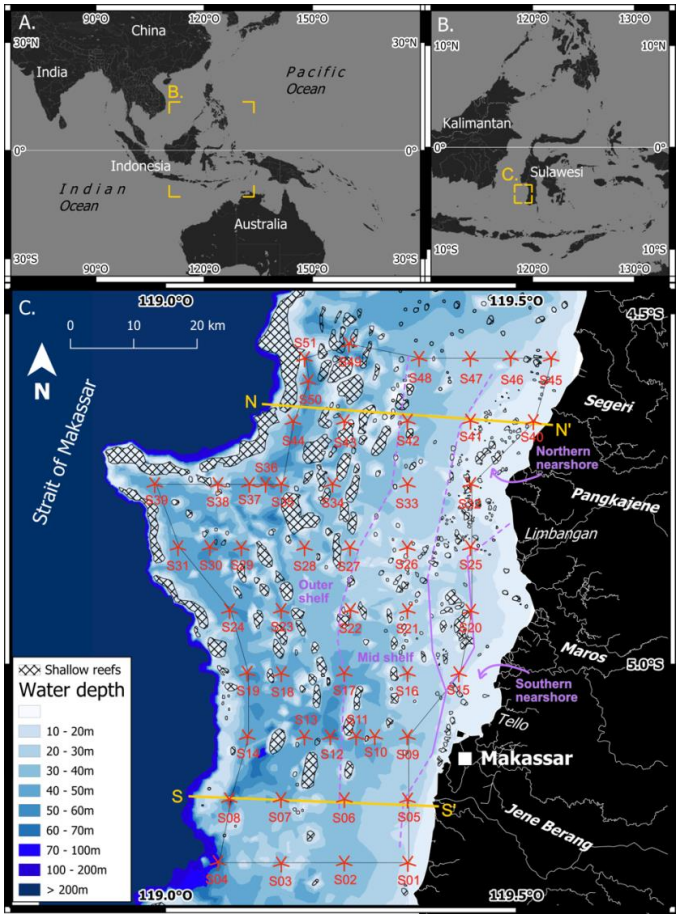

Figure 1. Study area and morphology of the Spermonde Archipelago, SW Sulawesi, Indonesia. (**A**) Location of Indonesia between the Indian and Pacific Oceans, with (**B**) near equatorial position of Sulawesi and the Spermonde Archipelago in the Southwest. (**C**) Bathymetry of the Spermonde shelf showing shallow reefs, major river systems, and zonation adjusted from Renema et al. (2001) and Kench & Mann (2017) to our findings with n = 51 sediment sampling stations indicated, as well as the locations of depth profiles across the northern (N-N') and southern (S-S') shelf (shown in Fig. 10). The bathymetric map is based on hydrographic charts from the Hydrographic and Oceanographic Centre of Indonesia (edition no. 9 from 18.12.2020; scale 1:100,000).

Numerous rivers discharge onto the shelf, including the Jene Berang in the south, the Tallo just north of Makassar, Maros in the central part, and the Pangkajene and Segeri rivers in the north (Fig. 1C, S1), delivering freshwater, nutrients, and terrigenous material to nearshore environments. Many islands in the Spermonde Archipelago are highly populated and rapid urban expansion of the city of Makassar and surrounding coastal areas has intensified anthropogenic pressures, leading to pronounced nearshore-offshore gradients in water quality, sedimentation, and reef condition (e.g., Cleary et al., 2005; Estradivari et al., 2025; Girard et al., 2022). Furthermore, recent geomorphological analyses further demonstrate spatial differentiation in island morphodynamics and sediment redistribution across the shelf (Sengupta et al., 2025).

The oceanographic conditions of the Spermonde Archipelago are governed by seasonally reversing monsoon winds (Fig. 2A, B) leading to fluctuating environmental conditions (Kench and Mann, 2017; Renema et al., 2001; Widagdo et al., 2022). During the dry season peaking in August, WNW winds from mainland Sulawesi promote

https://doi.org/10.5194/egusphere-2026-3460
Preprint. Discussion started: 5 August 2026

upwelling of cooler, nutrient-rich waters from the Strait of Makassar along the outer reef rim (Fig. 2C), butoffshore currents prevent a flow of the upwelled waters onto the shelf (Troelstra et al., 1996; Widagdo et al., 2022). Nearshore waters remain influenced by terrestrial discharge, leading to locally elevated chlorophyll a concentrations of >2 mg m^{-3} compared to 0.2-0.6 mg m^{-3} across the mid and outer shelf (Fig. 2E) and salinities on the shelf reaching up to 34.5‰ (Ilahude, 1970; Rosalina et al., 2024). In contrast, the wet season (December-January) is characterized by SE winds bringing increased precipitation and enhanced nutrient-rich fluvial input from the mountainous hinterland, generating strong nearshore-offshore gradients in chlorophyll a concentrations and sea-surface temperature (Fig. 2D, F) that disperse through southward currents (Cleary et al., 2005; Gordon et al., 1999; Kench and Mann, 2017; Fig 2A). Near river mouths, mean sea surface temperatures (SST) can reach 31°C, chlorophyll a concentrations exceed 4 mg m^{-3} and salinity may temporarily decrease to ~20‰, whereas mid- and offshore waters typically range between 31.5 and 32‰ (Ilahude, 1970; Renema and Troelstra, 2001). These combined gradients in hydrodynamics, nutrient availability, and anthropogenic influence create a marked spatial differentiation in reef communities and sedimentary environments across the shelf, providing an ideal setting to investigate cross-shelf variability in carbonate-producing assemblages.

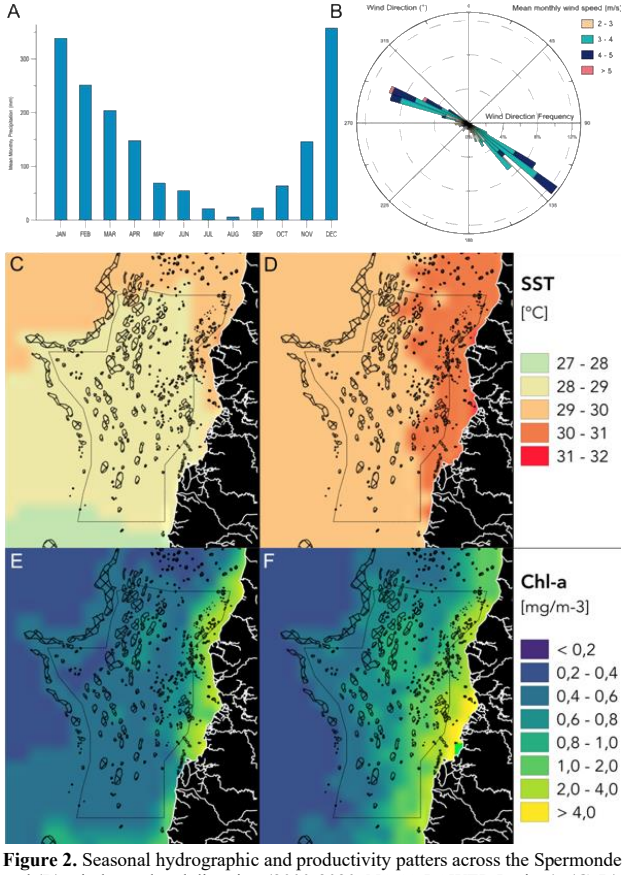

Figure 2. Seasonal hydrographic and productivity patters across the Spermonde Archipelago. (**A**) Mean monthly precipitation and (**B**) wind speed and direction (2000-2020; NASA POWER Project). (**C**, **D**) Multiannual average sea surface temperatures (SST) and (**E**, **F**) chlorophyll *a* concentrations. for August (**C**, **E**) August, i.e.; dry season, upwelling conditions); and January (**D**, **F**) January, i.e.; wet season, high precipitation), respectively (2003-2023; NASA MODIS Aqua, 4 km resolution). Data for C-F were obtained as monthly average netCDF files (NASA Ocean Biology Processing Group, 2015); multiannual averages were calculated using the *r.series* function in GRASS GIS (GRASS Development Team et al., 2017).

https://doi.org/10.5194/egusphere-2026-3460
Preprint. Discussion started: 5 August 2026

2 Materials & Methods

2.1 Field sampling

A total of n = 51 seafloor surface sediment samples was collected in July 2021 with a manually-operated van Veen grab deployed from a boat following a sampling grid targeting the deeper inter-reef zones while avoiding shallow reefs (Fig. 1C, Table S1). The grid spacing was 10 km, sampling points were relocated when reefs interfered. A PLASTIMO hand-held echo sounder Echotest II was used for depth measurements at the sampling sites.

2.2 Sediment analyses

Upon arrival in the laboratory, samples were oven-dried for 48 to 96 hours at 50°C and split into working and archive halves. To determine the content of calcium carbonate ($CaCO_3$) and total organic carbon (TOC) of bulk samples, dried subsamples of each surface sample were ground in a mortar. The $CaCO_3$ content was measured with an accuracy of 0.5% following Müller and Gastner (1971). The measured $CaCO_3$ content was calibrated by using a standardized artificial calcite powder with a known $CaCO_3$ content of 99.2% (manufacturer: *AppliChem GmbH, Germany*). The TOC content was measured using a *multiEA4000* macro-elemental analyser with an accuracy of 0.01%.

For grain-size analyses, all samples were washed in demineralized water and wet-sieved through a 63-µm sieve to remove salt and fine materials. Subsequently, the sediments were dried again and sieved into fractions following Wentworth (1922) with mesh widths ranging from 16 mm to 63 µm, and weighed. The content of sediment <63 µm was calculated through subtraction from the initial dry weight. Grain size statistics were calculated using GRADISTAT v9.1 (Blott and Pye, 2001).

2.3 Component analysis

The sediment components were analysed by point counting under a digital microscope (*Keyence VHX-5000*). The grain size fractions >2000 µm, 2000-1000 µm, 1000-500 µm, 500-250 µm and 250-125 µm were analysed until a total of 100 components per fraction was identified, resulting in a targeted total of 500 identified grains per sample. Grains <125 µm were not analysed. The relative proportions in each fraction were then used to calculate the weight percentage (wt%) of the analysed fractions. The resulting proportions of components thus represent the proportions in the sediment fraction >125 µm.

2.4 Foraminiferal analysis and FoRAM Index

Benthic foraminiferal assemblages were analysed to characterize spatial changes in functional responses to environmental gradients across the shelf, expressed as the FoRAM Index (FI; Hallock et al., 2003). Due to their relatively short life spans and the sensitivity of their tests to post-mortem alteration, analyses focused on well-preserved tests provide a robust proxy for near-surface environmental conditions.

A subsample of each sample was sieved at 125 µm, and a minimum of 150 tests of benthic foraminifers was identified to genus level as recommended by Prazeres et al. (2020) from all coarser fractions. Tests were grouped in three functional categories according to Hallock et al. (2003): symbiont-bearing, small heterotrophic, and stress-tolerant taxa. FI values were calculated according to Eq. (I):

$$FI = (10 \times P_s) + (2 \times P_h) + P_o \quad \text{(I)},$$

https://doi.org/10.5194/egusphere-2026-3460
Preprint. Discussion started: 5 August 2026

where P_s, P_h, and P_o represent the relative proportion of symbiont-bearing, heterotrophic, and stress-tolerant taxa (Table 1), respectively.

Table 1. Genera of benthic foraminifera identified and their respective functional groups for the calculation of the FoRAM Index. The order of listing follows the total counts in the data set. Functional groups are based on previous studies (Fajemila et al., 2015; Schmidt et al., 2018; Uthicke et al., 2009).

FoRAM Index Functional Group	Genus
Symbiont-bearing	*Amphistegina, Operculina, Peneroplis, Calcarina, Pararotalia, Neorotalia, Parasorites, Heterostegina, Nummulites, Baculogypsina, Dendritina, Sorites, Borelis, Alveolinella, Planoperculina*
Heterotrophic	*Quinqueloculina, Cibicidoides, Discorbinella, Cibicides, Textularia, Spiroloculina, Neoeponides, Ammomassilina, Cornuspira, Cancris, Homotrema, Triloculina, Reophax, Spirosigmoilina, Lagena, Cymbaloporetta, Planorbulina, Siphoniferoides, Pyrgo, Parahauerina*
Stress-tolerant	*Nonion, Ammonia, Elphidium, Bolivinita, Rotaliammina, Reusella*

The FI was originally developed as an indicator of reef growth potential in shallow-water environments (Hallock, 2012; Hallock et al., 2003) and its application typically excludes fine-grained samples (Prazeres et al. (2020). Here, fine-grained samples from inter-reef settings were retained, as low FI values in these samples likely reflect genuinely unfavourable photic and substrate conditions associated with chronic terrestrial input, rather than a methodological artifact. The FI is therefore used as a relative proxy for cross-shelf gradients in benthic foraminiferal functional composition, with FI thresholds (>4 suitable, 4-2 marginal, and <2 unsuitable) interpreted accordingly rather than as absolute predictors of reef development potential

2.5 Spatial data interpolation & statistical analysis

Spatial distribution maps of grain-size fractions, skeletal components and geochemical variables, as well as FI values, were generated in QGIS using interpolated surfaces from sample point data. Raster outputs were clipped to the shelf extent shown in Fig. 1. To identify different sediment facies with a statistically valid approach, cluster analysis in the software PAST v4.15 (Hammer et al., 2001) with Euclidian distances and Ward's method (Ward, 1963) was applied. These multivariate statistical analyses were performed exclusively on sedimentological and geochemical parameters (relative proportions grain size fractions, $CaCO_3$ content, and skeletal component proportions) to define facies clusters independent of foraminiferal assemblage compositions.
After identification of clusters, the means of each parameter were calculated and used to designate facies by their biogenic (Lees, 1975; Lees and Buller, 1972) and textural composition (Dunham, 1962). Furthermore, Principal Component Analysis (PCA) was used to infer associations of the foraminifera data with spatial, geochemical and textural characteristics of the sediment by plotting correlation matrices as biplots.

2.6 Bathymetric mapping, remote sensing data and synthesis

Bathymetric data of the Spermonde shelf were derived from hydrographic charts of the Indonesian Hydrographic and Oceanographic Centre (1:100,000; edition 9, 18.12.2020). Charts were georeferenced in QGIS v3.18, and depth contours were digitized to generate a digital elevation model using a Triangulated Irregular Network (TIN) interpolation. Seasonal hydrographic conditions were characterized using satellite-derived datasets. Monthly precipitation and wind data (2000-2020) were obtained from the National Aeronautics and Space Administration (NASA) Langley Research Center (LaRC) Prediction of Worldwide Energy Resource (POWER) project. Sea

https://doi.org/10.5194/egusphere-2026-3460
Preprint. Discussion started: 5 August 2026

surface temperature (SST) and chlorophyll *a* concentrations (2003-2023) were retrieved from NASA Ocean Color Aqua-MODIS (4 km resolution) as monthly netCDF files. Multiannual monthly means were calculated using the *r.series* function in GRASS GIS (Neteler et al., 2012).

To contrast representative northern and southern shelf conditions in profiles, samples were grouped into two spatial sectors: a southern sector (S01-S14) and a northern sector (S32-S51), corresponding to the latitudinal end-members of the sampling grid. Within each sector, samples were further assigned to cross-shelf zones (nearshore, inner mid-shelf, outer mid-shelf, offshore) based on their spatial position relative to the shelf zonation. Mean values of all sedimentological, geochemical, and foraminiferal parameters were calculated per zone within each sector and plotted at the mean cross-shelf distance of the corresponding samples to construct the representative shelf profiles. Three spatially clustered outer-shelf samples from the northern sector (S36, S38, S39) were excluded, as they represent a localised seaward shelf extension confined to the southernmost transect of the northern corridor and would disproportionately bias the offshore zone mean (Fig. 1C).

3 Results

3.1 Grain Size Distribution

The surface samples consist mainly of a mixture of mud (<0.063 mm) and sand (0.063 to 2 mm) fraction while coarser components are rare (Fig. 3; Table 3, Table S2).

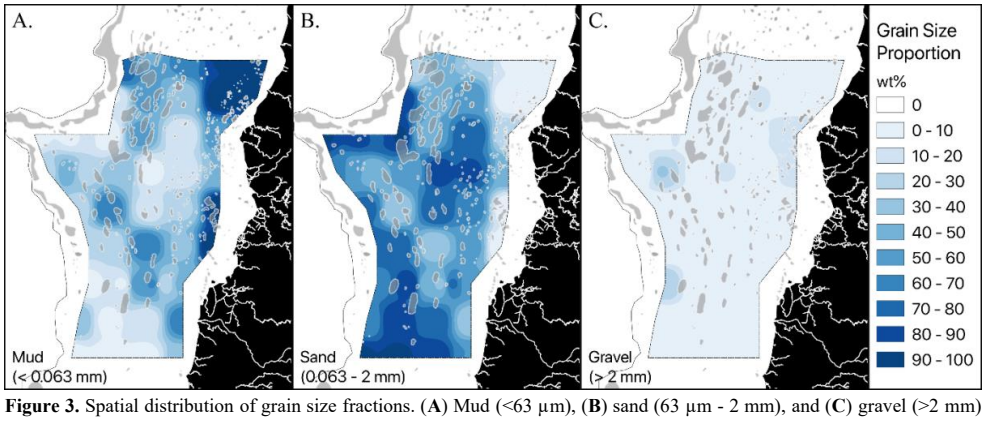

Figure 3. Spatial distribution of grain size fractions. (**A**) Mud (<63 µm), (**B**) sand (63 µm - 2 mm), and (**C**) gravel (>2 mm) proportions in surface sediments; based on TIN interpolations.

Mud-rich sediments (>90 weight percentage 'wt%') dominate the nearshore zone on the central shelf and in the northern shelf they locally extend to the mid shelf (Fig 3A). On most of the mid and outer shelf, sand-fraction dominated sediments prevail (70 to 80 wt%, Fig. 3B), except for some mud-rich mid-shelf areas where the sand fraction contributes around 30 wt% (e.g., S11, S17 and S48). Gravel (>2 mm) generally accounts for <10 wt% (Fig. 3C) of the sediment, with the locally highest contents being 20-30 wt% in two outer-shelf samples.

3.2 $CaCO_3$ and TOC contents

The $CaCO_3$ content ranges between 20 and 92 wt% and generally increases with distance from the mainland, whereas the TOC content follows the opposite trend (Fig. 4; Table 3, Table S1).

https://doi.org/10.5194/egusphere-2026-3460
Preprint. Discussion started: 5 August 2026

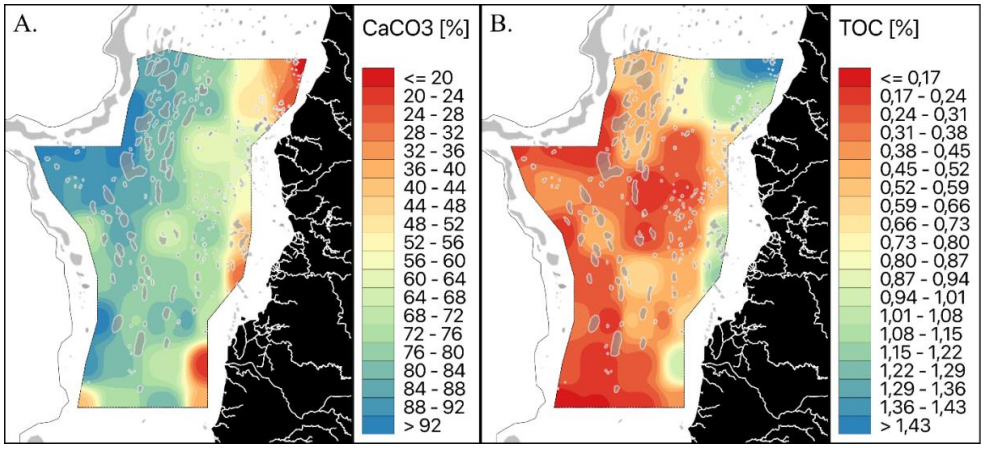

Figure 4. Spatial distribution of calcium carbonate ($CaCO_3$) and total organic carbon (TOC) contents. (**A**) $CaCO_3$, and (**B**) TOC percentages in surface sediments; based on TIN interpolations.

The lowest $CaCO_3$ values are measured in samples from both the northern and southern nearshore zone (Fig. 4A). On the mid-shelf, $CaCO_3$ increases with distance from the mainland to a maximum of 60-80%, with a more gradual offshore rise in the northern compared to the central and southern shelf. Outer shelf sediments have consistently higher $CaCO_3$ contents (commonly >90%), apart from the southernmost outer-shelf sample S4, which contains relatively little carbonate (43%).

TOC values are highest in the northern nearshore zone (1.2 to 1.4%), and also are elevated (>1.0%) in the central and southern nearshore zone (Fig. 4B). TOC contents decrease markedly offshore and are generally below 0.3% on the mid to outer shelf, with only slightly higher values (0.5 to 0.6%) measured on the mid shelf.

3.3 Sedimentary components

Across all 51 samples, the dominant components in the fractions >125 µm are benthic foraminifers (mean 36.6 wt%), followed by bivalves (21.4 wt%), gastropods (11.8 wt%), and echinoderms (6.7 wt%) (Tables 2, 3 and Table S3). The skeletal grains show a varying degree of alteration through bioerosion, breakage or abrasion, ranging from pristine (“fresh”), over slightly abraded and/or fragmented, to a strongly overprinted eroded habitus. Non-skeletal grains were rarely observed. and sorting is generally poor to very poor (according to descriptions of Folk and Ward; Table S2), suggesting low-energy depositional conditions with limited physical sorting and predominantly (par)autochthonous deposition.

https://doi.org/10.5194/egusphere-2026-3460
Preprint. Discussion started: 5 August 2026

Table 2. Identified skeletal and non-skeletal components in seafloor samples from the Spermonde Archipelago, with the number of samples in which they were present in, the minimum and maximum proportion, and the average relative proportion displayed separately.

Component	Number of samples present in	Minimum [wt%]	Maximum [wt%]	Average [wt%]
Benthic foraminifers	51 (100%)	1.2	66.8	36.6
Bivalves	51 (100%)	3.9	78.0	21.4
Gastropods	51 (100%)	0.2	21.4	11.8
Echinoderms	51 (100%)	0.1	17.1	6.7
Bryozoans	41 (80.4%)	0	20.4	4.1
Red Algae	36 (70.6%)	0	18.2	2.7
Ostracods	50 (98.0%)	0	10.8	2.0
Scaphopods	50 (98.0%)	0	7.5	1.7
Halimeda	30 (58.8%)	0	9.8	1.7
Planktic foraminifers	36 (70.6%)	0	9.7	1.2
Sponge needles	32 (62.7%)	0	5.4	1.0
Corals	41 (70.6%)	0	5.6	1.1
Serpulid tubes	33 (64.7%)	0	2.8	0.5
Balanids	29 (56.9%)	0	2.0	0.3
Authigenic crystals	16 (31.4%)	0	61.7	5.6
Siliciclasts	20 (39.2%)	0	33.5	1.1
Siderites	7 (13.7%)	0	12.7	0.6

3.3.1 Skeletal components

The relative contribution of skeletal components varies systematically across the shelf (Fig. 5, Table 3). Benthic foraminifers show lowest abundances (<10 wt%) in the northern nearshore zone, but increase markedly on the mid and outer shelf, where they commonly contribute 30-40 wt%, with local maxima of >60 wt% (Fig. 5A). In the coarser fractions, intact, slightly fragmented or altered photosymbiotic larger benthic foraminifers dominate (mainly *Amphistegina, Operculina* and *Elphidium* spp.), in the finer fractions intact smaller specimens are present, mainly of the orders Rotaliida and Milliolida, as well as fragments that did not allow further identification.

Bivalves dominate nearshore settings (locally >60 wt%) and decrease progressively offshore to ~30 wt% at mid-shelf, decreasing below 10 wt% (Fig. 5B). Gastropods occur throughout the shelf (Fig. 5C), with lowest abundances in the nearshore zones (5-10 wt%) and increase towards the mid and outer shelf, where they are common components reaching 10 to 20 wt%. Echinoderm remains (spines and other skeletal fragments from echinoids, platy fragments from holothuroids and asteroids) are minor to common constituents in all samples (Fig. 5D), with local elevations in the nearshore to mid shelf zones (15-20 wt%), but tend to decrease to <5 wt% on the outer shelf. Bryozoans were observed in branching and encrusting forms, of which the latter mainly use larger benthic foraminifers as substrate. They contribute less than 5 wt% on the mid shelf and increase towards the outer shelf, where they commonly contribute ~10 wt% and partly up to 20 wt% (Fig. 5E). Calcifying red algae and fragments of the calcifying green alga *Halimeda* follow a similar offshore-increasing trend as rare to common

https://doi.org/10.5194/egusphere-2026-3460
Preprint. Discussion started: 5 August 2026

constituents in seafloor sediments of the outer shelf and scattered on the mid shelf, showing concentrations of 5 to 10 wt% and ~5 wt%, respectively (Fig. 5F, I).

Minor constituents include ostracod shells, which are most abundant in the northern nearshore zone (5-10 wt%, Fig. 6G), as well as elongated tests of scaphopods, predominantly present on the mid shelf and locally in nearshore zones (Fig. 5H). Remains of corals were observed in small proportions in some mid- and outer-shelf samples (<5 wt%, Fig. 5J). Rare constituents are planktonic foraminifers, sponge needles, and serpulid tubes, whose occurrence is limited to the outer shelf (Fig. 5K, L, M), while balanids were observed only in the southern nearshore zone (Fig. 5N).

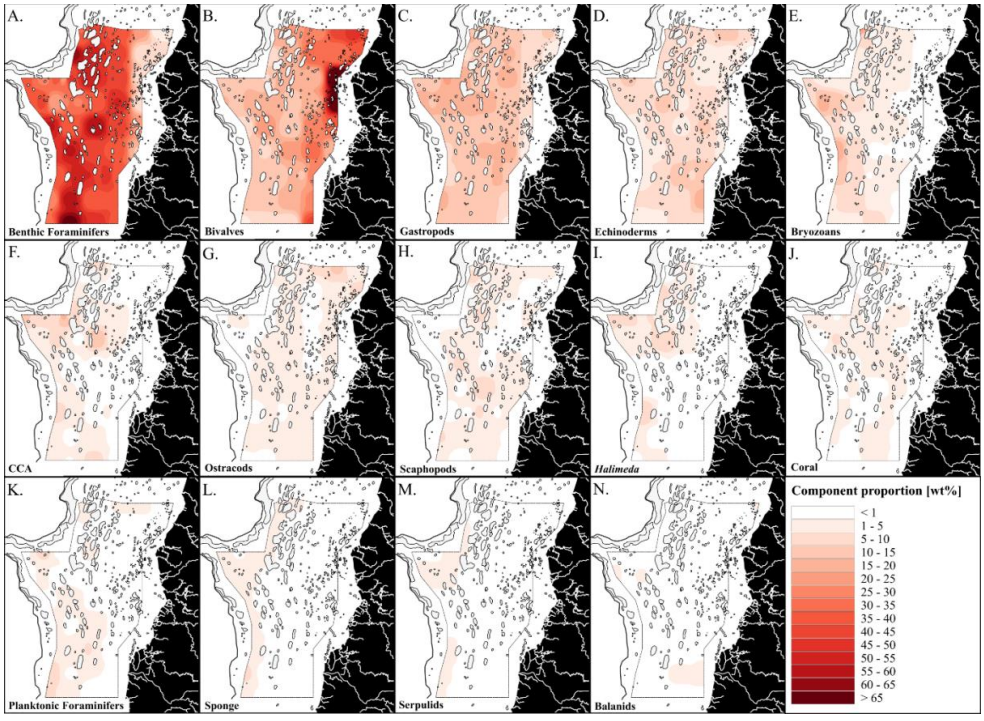

Figure 5. Distributions of skeletal components across the Spermonde Archipelago. Proportions of (**A**) benthic foraminifers, (**B**) bivalves, (**C**) gastropods, (**D**) echinoderms, (**E**) bryozoans, (**F**) red algae, (**G**) ostracods, (**H**) scaphopods, (**I**) *Halimeda*, (**J**) corals, (**K**) planktonic foraminifers, (**L**) sponges, (**M**) serpulids and (**N**) balanids in grain size fractions between 125 and 2000 µm of surface sediments.

3.3.2 Non-Skeletal Components

Siliciclasts are generally rare (only seven samples >1 wt%, Fig. 6B, Table 3), but reach an exceptional contribution of 33.5 wt% in the southernmost outer-shelf sample S04. Siderite concretions of up to 2 mm occur sporadically (Appendix A2-4) on the mid shelf, locally contributing up to 5 wt% (Fig. 6C).

Authigenic gypsum crystals (Appendix A1), are limited to mud-rich (>95 wt% of grains <0.063 µm) nearshore samples, where they may have formed during the drying procedure in the laboratory (>40 wt%, Fig. 6A) (e.g., S40, S45; Table 3).

https://doi.org/10.5194/egusphere-2026-3460
Preprint. Discussion started: 5 August 2026

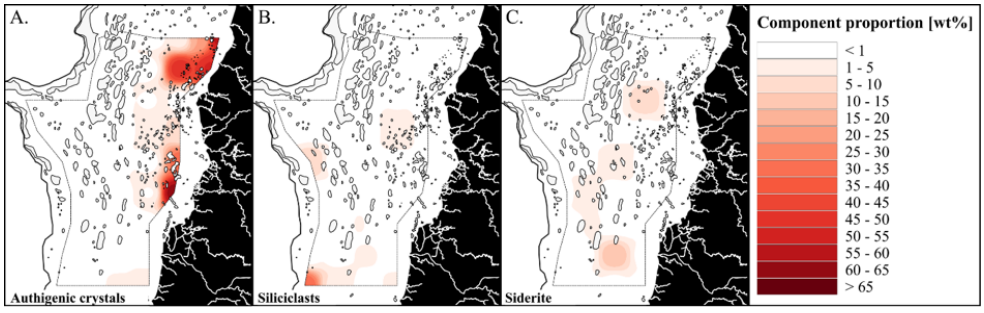

Figure 6. Distribution of non-skeletal grains across the Spermonde Archipelago. Proportions of (**A**) authigenic crystals, (**B**) siliciclasts and (**C**) siderite in grain size fractions between 125 and 2000 µm of surface sediments.

3.4 Foraminiferal assemblages and FoRAM Index

A total of 41 different genera of benthic foraminifera were identified (Tables 1, 3), with *Amphistegina*, *Nonion*, *Ammonia*, *Cibicidoides*, *Quinqueloculina*, *Operculina, and Elphidium* representing the seven most dominant taxa across the shelf (in decreasing order of total relative abundance). Clear cross-shelf gradients are evident in functional group compositions and corresponding FI values (Fig. 7). In the central and northern nearshore zones, assemblages are mainly dominated by stress-tolerant genera (mostly *Nonion*, *Ammonia*, and *Elphidium*), resulting in low FI values between 1.0 and 1.5 (Fig. 7A, B).

Across the southern nearshore zone northward and mid-shelf, benthic foraminifer assemblages shift to a mix of heterotrophic taxa (mainly *Quinqueloculina* and *Cibicidoides*), with some subordinate stress-tolerant taxa. Correspondingly, FI values mainly range between 2 and 4 (Fig. 7A, C). On the outer shelf, symbiont-bearing genera, particularly *Amphistegina* and *Operculina*, increase markedly to higher abundances, which results in FI values between 4 and 7 in these settings (Fig. 7A, D). Although the highest FI values occur primarily on the mid-shelf, values <4 extent into deeper inter-reef habitats (>50 m water depth, Table S4).

https://doi.org/10.5194/egusphere-2026-3460
Preprint. Discussion started: 5 August 2026

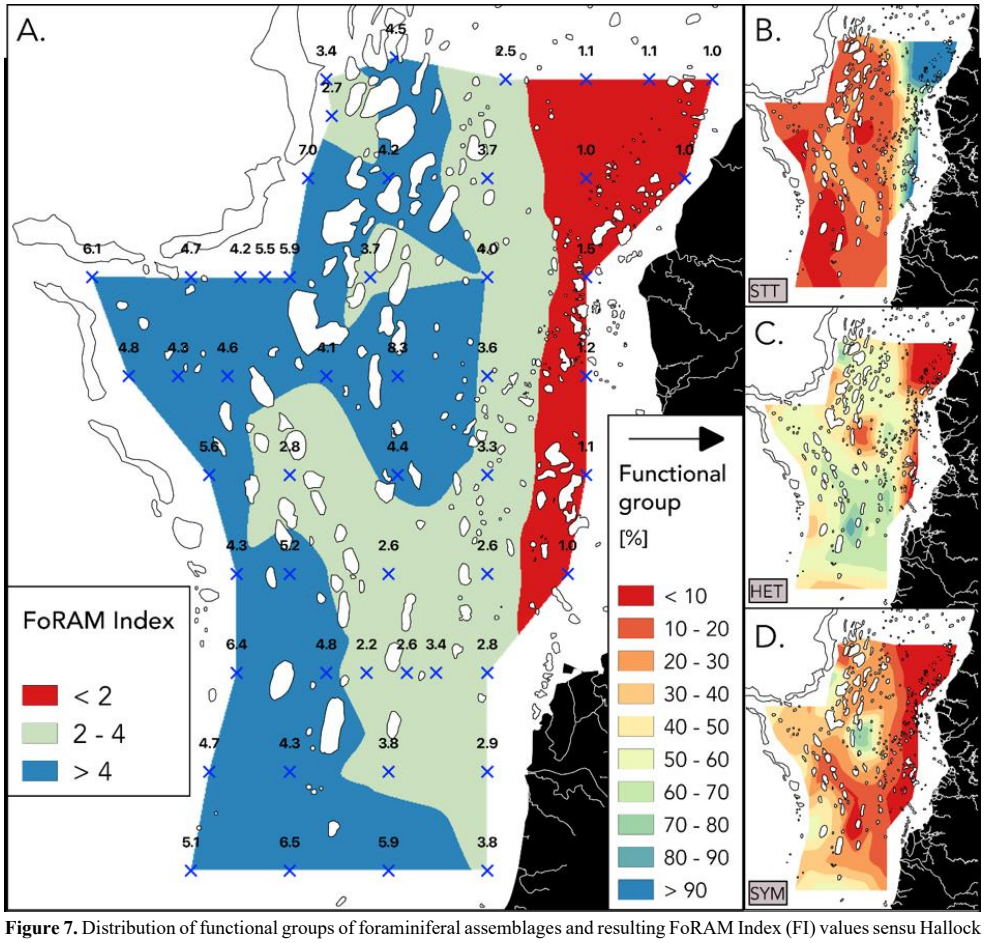

Figure 7. Distribution of functional groups of foraminiferal assemblages and resulting FoRAM Index (FI) values sensu Hallock et al. (2003) across the Spermonde shelf. (**A**) Calculated FI values, based on percentages of (**B**) stress-tolerant (STT), (**C**) heterotrophic (HET), and (**D**) symbiont-bearing (SYM) taxa.

3.5 Sedimentary facies

Euclidian cluster analysis of grain-size distribution, skeletal component, and geochemical parameters identified six facies across all seafloor sediments (Fig. 8). The following proportions are mean values, with standard deviations provided in Table 3.

https://doi.org/10.5194/egusphere-2026-3460
Preprint. Discussion started: 5 August 2026

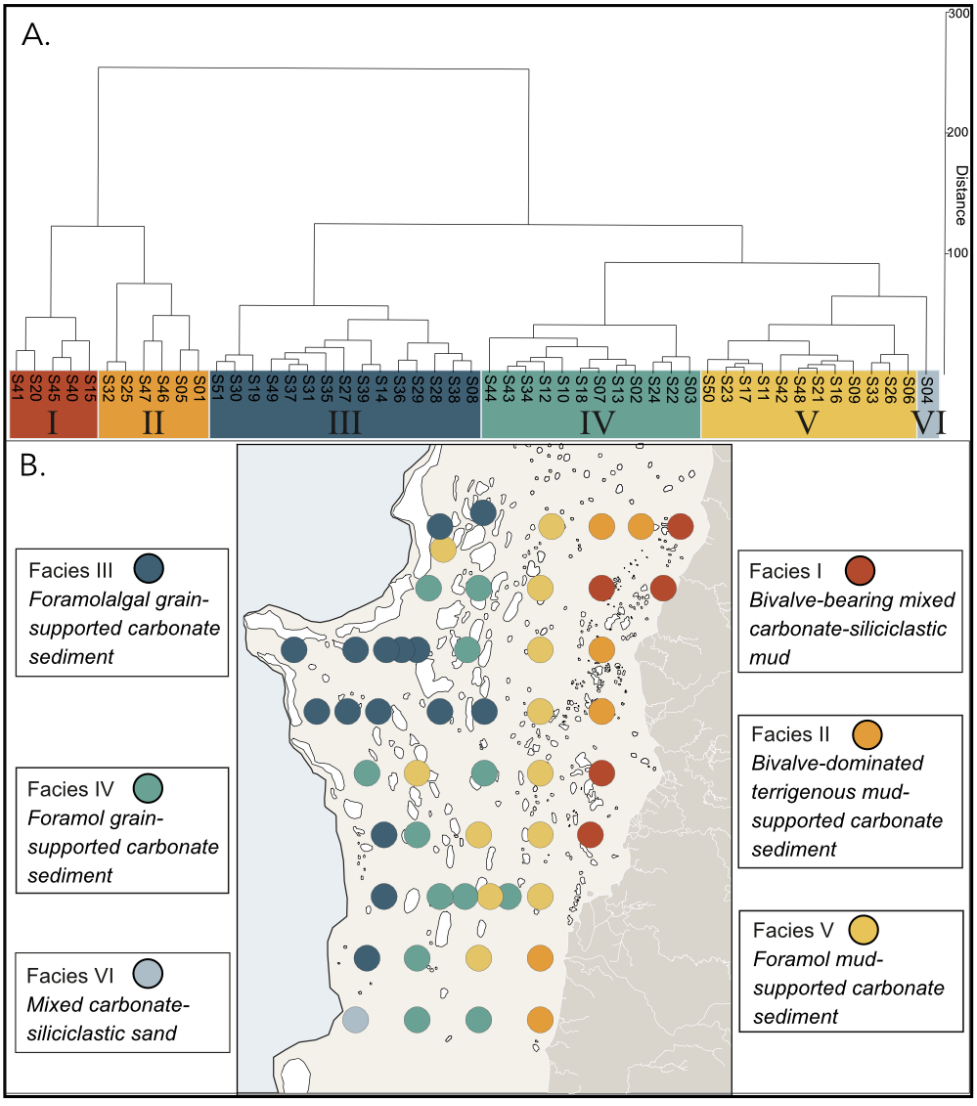

Figure 8. Sedimentary facies across the Spermonde shelf. (**A**) Dendrogram of Euclidean cluster analysis based on grain-size distribution, skeletal components, and geochemical parameters, distinguishing six facies (I–VI). (**B**) Spatial distribution of the identified facies across the study area. Facies I and II are confined to nearshore settings, whereas Facies III–V dominate the mid and outer shelf. Facies VI is represented by a single outer-shelf sample.

Facies I: Bivalve-bearing mixed carbonate-siliciclastic mud (n = 5)

Facies I is restricted to the central and northern nearshore zone at shallow depths (6.0 ± 3.3 km from the mainland, 13.5 ± 5.7 m depth). It is characterized by a high mud content of 97.4 wt%, low $CaCO_3$ values (33.8%) and an elevated TOC content (1.2%). Bivalves (31.1 wt%) form the main skeletal component, benthic foraminifers (10.8 wt%) and ostracods (3.3 wt%) are rare components, while authigenic gypsum crystals are abundant in the coarse fraction (49.2 wt%).

https://doi.org/10.5194/egusphere-2026-3460
Preprint. Discussion started: 5 August 2026

Facies II: Bivalve-dominated terrigenous-bearing mud-supported carbonate sediment (n = 6)

Facies II is also confined to the nearshore zone (20.3 ± 8.7 m water depth). It contains a higher $CaCO_3$ content (45.6%), more of the sand fraction (29.1 wt%) and gravel (6.2 wt%) compared to facies I, but remains mud-rich overall with a lower TOC (0.9%). Bivalves strongly dominate the skeletal components (51.3 wt%), while benthic foraminifers are common (19.3 wt%).

Facies III: Foramolalgal grain-supported carbonate sediment (n = 15)

Facies III is predominantly found on the outer shelf (8.6 ± 5.8 km from the platform rim) and in deeper inter-reef settings (47.3 ± 9.9 m). Sediments are mainly sand-dominated (67.0 wt%), $CaCO_3$-rich (89.1%) and low in TOC (0.3%). Benthic foraminifers are the dominant component (35.0 wt%), accompanied by gastropods (14.7 wt%), bivalves (14.0 wt%), bryozoans (7.9 wt%) and calcareous algae (red algae: 7.4 wt%; *Halimeda*: 4.5 wt%). Corals contribute minorily (2.1 wt%).

Facies IV: Foramol grain-supported carbonate sediment (n = 12)

Facies IV is present across the mid and outer shelf (41.2 ± 5.8 m depth) and is defined by a high sand (73.0%) and elevated $CaCO_3$ content (80.5%). Mud (23.9%) and TOC contents (0.3%) are low. Benthic foraminifers dominate (54.8 wt%), while gastropods (12.3 wt%), bivalves (10.9 wt%) and bryozoans (5.1 wt%) are common but subordinate components. Compared to facies III, calcifying red algae (1.7 wt%) and *Halimeda* (1.2 wt%) are minor.

Facies V: Foramol mud-supported carbonate sediment (n = 12)

Facies V occupies mainly mid-shelf to nearshore settings (37.6 ± 9.6 m depth) and sediments are mixed sand-mud compositions (51.7 and 43.1 wt%, respectively) with intermediate $CaCO_3$ content (76.3%) and low TOC (0.5%). Benthic foraminifers remain dominant (40.3 wt%), accompanied by common bivalves (23.8 wt%) and gastropods (14.0 wt%).

Facies VI: Mixed carbonate-siliciclastic sand (n = 1)

Facies VI is represented by a single outer-shelf sample (S04; 68.8 m) characterised by elevated siliciclastic input (33.5 wt%) and comparatively low $CaCO_3$ content (43.3%). Skeletal components are dominated by benthic foraminifers (32.6 wt%) with subordinate contributions from gastropods (12.6 wt%).

Table 3. Overview of all samples according to their facies across the Spermonde Archipelago, based on grain-size distribution (GRV = gravel, SAN = sand, MUD = mud), carbonate content ($CaCO_2$), and skeletal component composition (COR = coral, RDA = red algae, HAL = *Halimeda*, BFO = benthic foraminifers, PFO = planktic foraminifers, GPO = gastropods, BIV = bivalves, ECH = echinoderms, BRY = bryozoans, SER = serpulids, BAL = balanids, SCA = scaphopods, SPO = sponge, OST = ostracods, SIL = siliciclasts, SID = siderite, ACR = authigenic crystals), along with their respective total organic carbon content (TOC), descriptions of their spatial distribution on the shelf (Depth = sample water depth, DML = sample distance from mainland, and DSOM = sample distance from the Strait of Makassar), and proportions of functional groups of benthic foraminifera with resulting FoRAM Index values (Ps = symbiont-bearing foraminifers, Ph = heterotrophic foraminifers, Po = stress-tolerant foraminifers, FI = FoRAM Index).

https://doi.org/10.5194/egusphere-2026-3460
Preprint. Discussion started: 5 August 2026

Sample	Depth	DML	DSOM	GRV	SAN	MUD	$CaCO_3$	TOC	COR	RDA	HAL	BFO	PFO	GPO	BIV	ECH	BRY	SER	BAL	SCA	SPO	OST	SIL	SID	ACR	Ps	Ph	Po	FI
[]	[m]	[km]	[km]	[wt%]	[wt%]	[wt%]	[%]	[%]	[wt%]	[wt%]	[wt%]	[wt%]	[wt%]	[wt%]	[wt%]	[wt%]	[wt%]	[wt%]	[wt%]	[wt%]	[wt%]	[wt%]	[wt%]	[wt%]	[wt%]	[%]	[%]	[%]	[]
F I	*Bivalve-bearing mixed carbonate-siliciclastic mud*																												
S15	14.0	5.4	38.4	0.0	2.0	98.0	30.6	1.2	0.0	0.0	0.8	14.9	0.3	1.6	15.4	2.2	0.0	0.0	0.0	1.7	0.0	1.5	0.0	0.0	61.7	0.0	2.6	97.4	1.0
S20	17.1	8.2	41.6	0.0	2.7	97.3	43.3	1.0	0.0	0.0	0.0	22.7	0.0	3.1	35.1	2.4	0.0	0.2	0.0	0.7	1.0	3.3	0.0	0.0	31.5	0.0	5.0	95.0	1.1
S40	4.5	1.6	40.0	0.5	1.5	98.0	27.7	1.0	0.0	0.1	0.1	6.8	0.1	1.1	35.2	0.6	0.0	0.0	0.1	0.1	0.0	5.5	0.1	0.0	50.2	0.0	1.9	98.1	1.0
S41	19.2	10.1	30.1	0.0	2.4	97.6	51.1	1.1	0.0	0.0	0.0	7.9	0.6	5.5	30.5	3.9	0.0	0.0	0.0	0.2	0.0	4.6	0.0	0.0	46.8	0.0	2.0	98.0	1.0
S45	12.6	4.5	42.7	1.7	2.0	96.3	16.0	1.5	0.0	0.0	0.0	1.2	0.0	0.2	39.2	0.1	0.0	0.0	1.7	0.0	0.0	1.5	0.0	0.0	56.0	0.0	0.0	100.0	1.0
MEAN	**13.5**	**6.0**	**38.6**	**0.4**	**2.1**	**97.4**	**33.7**	**1.2**	**0.0**	**0.0**	**0.2**	**10.7**	**0.2**	**2.3**	**31.1**	**1.8**	**0.0**	**0.0**	**0.4**	**0.6**	**0.2**	**3.3**	**0.0**	**0.0**	**49.2**	**0.0**	**2.3**	**97.7**	**1.0**
STDDEV	**5.6**	**3.3**	**5.0**	**0.7**	**0.5**	**0.7**	**13.7**	**0.2**	**0.0**	**0.0**	**0.3**	**8.3**	**0.2**	**2.1**	**9.3**	**1.5**	**0.0**	**0.1**	**0.7**	**0.7**	**0.4**	**1.8**	**0.0**	**0.0**	**11.4**	**0.0**	**1.8**	**1.8**	**0.0**
F. II	*Bivalve-dominated terrigenous mud-supported carbonate sediment*																												
S01	12.8	2.9	30.8	3.2	59.9	36.9	37.9	0.4	0.2	0.0	0.0	38.8	0.0	4.7	41.0	6.9	0.0	0.0	0.5	0.2	0.0	3.0	1.4	0.0	3.2	25.8	43.2	31.0	3.8
S05	28.3	3.7	31.1	1.2	33.1	65.7	22.4	1.0	0.5	0.1	0.0	38.7	0.7	9.3	25.6	17.1	0.5	0.0	2.0	0.9	0.0	4.5	0.1	0.0	0.0	13.7	67.3	19.0	2.9
S25	17.3	6.9	45.0	13.6	46.3	40.2	59.3	0.6	0.2	0.0	0.2	6.4	0.0	6.4	72.2	3.1	0.0	0.2	0.7	0.7	0.0	3.3	0.0	0.0	6.6	0.0	16.0	84.0	1.2
S32	9.9	5.3	32.9	18.7	24.0	57.3	64.7	0.7	0.0	0.0	0.0	8.0	0.2	4.1	78.0	4.1	0.0	0.2	0.8	1.7	0.0	2.7	0.2	0.0	0.0	1.3	34.0	64.7	1.5
S46	21.6	10.1	36.3	0.5	2.0	97.6	34.5	1.5	0.0	0.5	0.0	2.5	0.9	11.6	49.5	9.4	0.0	0.4	0.0	2.2	0.0	2.9	0.0	0.0	20.0	0.7	0.7	98.7	1.1
S47	32.0	14.8	30.1	0.1	9.5	90.3	54.5	1.3	0.0	0.0	0.0	21.4	1.3	5.6	41.7	14.6	0.0	0.3	0.0	1.3	0.2	10.8	0.0	0.0	2.8	0.0	6.5	93.5	1.1
MEAN	**20.3**	**7.3**	**34.4**	**6.2**	**29.1**	**64.7**	**45.5**	**0.9**	**0.1**	**0.1**	**0.0**	**19.3**	**0.5**	**7.0**	**51.3**	**9.2**	**0.1**	**0.2**	**0.7**	**1.2**	**0.0**	**4.5**	**0.3**	**0.0**	**5.4**	**6.9**	**28.0**	**65.1**	**1.9**
STDDEV	**8.7**	**4.5**	**5.7**	**7.9**	**21.9**	**25.2**	**16.4**	**0.4**	**0.2**	**0.2**	**0.1**	**16.3**	**0.5**	**2.9**	**20.1**	**5.7**	**0.2**	**0.2**	**0.7**	**0.7**	**0.1**	**3.1**	**0.5**	**0.0**	**7.6**	**10.7**	**25.2**	**33.4**	**1.1**
F. III	*Foramolalgal grain-supported carbonate sediment*																												
S08	73.6	31.7	5.0	1.3	62.3	36.4	89.5	0.3	1.1	5.2	3.1	27.1	9.6	16.5	12.1	5.1	4.8	1.4	0.3	5.1	5.4	3.2	0.0	0.0	0.0	35.3	54.7	10.0	4.7
S14	41.3	30.4	5.1	27.3	66.1	6.6	93.4	0.3	2.3	10.6	9.6	37.6	1.0	8.0	10.0	3.5	11.2	2.0	0.4	0.3	3.4	0.2	0.0	0.0	0.0	56.3	34.7	9.0	6.4
S19	50.2	34.1	5.0	1.5	77.8	20.6	79.3	0.3	0.2	1.7	0.3	47.8	1.7	9.5	10.5	4.1	18.7	0.2	0.1	1.7	2.1	1.3	0.0	0.0	0.0	30.9	52.7	16.4	4.3
S27	27.6	25.8	22.8	10.2	83.4	6.4	80.7	0.2	4.6	14.4	4.3	37.4	0.0	16.7	11.9	4.6	2.1	0.4	0.0	0.6	0.9	1.3	0.5	0.1	0.3	80.3	12.7	7.0	8.4
S28	37.5	32.9	18.8	8.1	53.1	38.8	86.1	0.4	3.4	1.0	9.8	29.9	0.2	16.6	19.6	11.3	5.2	0.0	0.4	1.5	0.0	1.1	0.0	0.0	0.0	29.4	47.2	23.3	3.1
S29	46.7	42.4	13.3	30.3	42.4	27.3	90.9	0.4	5.2	8.8	3.2	21.9	0.5	16.3	18.4	6.0	12.7	2.8	1.1	1.1	1.3	0.8	0.0	0.0	0.0	33.1	57.1	9.7	4.6
S30	46.3	47.3	9.6	3.6	50.7	45.8	87.5	0.4	0.2	1.6	1.5	41.0	1.8	14.9	10.2	6.8	17.5	1.2	0.3	0.6	2.0	0.5	0.0	0.0	0.0	29.9	59.8	10.3	4.3
S31	50.5	52.2	4.9	4.6	68.8	26.5	91.2	0.4	0.6	4.6	5.0	36.5	0.0	16.9	15.2	6.8	7.2	1.6	1.5	0.5	3.4	0.3	0.0	0.0	0.0	36.9	52.0	11.2	4.8
S35	42.4	35.2	8.4	4.3	92.4	3.3	95.8	0.2	1.8	8.9	4.8	45.8	0.0	19.8	9.6	4.2	1.3	1.2	0.2	0.3	2.0	0.0	0.0	0.0	0.0	49.8	39.3	10.9	5.9
S36	49.9	37.7	7.3	13.4	80.7	5.9	93.9	0.2	5.6	18.2	6.1	21.2	1.0	18.1	14.2	5.9	4.0	2.2	0.5	1.0	1.9	0.3	0.0	0.0	0.0	45.0	45.0	9.9	5.5
S37	49.9	40.2	5.7	6.2	77.7	16.0	89.5	0.2	0.2	7.1	2.6	38.1	0.8	21.4	15.0	6.8	2.0	1.2	0.7	1.0	2.1	0.8	0.3	0.0	0.0	29.1	53.9	17.0	4.2
S38	52.7	45.1	4.6	7.1	85.3	7.5	93.4	0.2	2.7	9.6	7.7	29.1	6.0	11.4	14.4	11.2	3.6	0.6	0.3	0.2	0.8	2.5	0.0	0.0	0.0	35.1	53.0	11.9	4.7
S39	45.8	55.1	3.2	3.5	90.9	5.6	92.9	0.2	2.0	11.2	7.3	37.5	0.5	10.1	11.7	8.3	5.0	0.7	0.0	0.8	4.6	0.2	0.0	0.0	0.0	53.0	33.8	13.2	6.1
S49	41.3	32.5	11.6	5.2	47.0	47.9	87.5	0.5	1.7	6.8	2.2	41.0	0.5	13.1	21.5	5.8	2.3	0.7	0.5	1.0	2.2	0.5	0.2	0.0	0.0	33.8	45.5	20.8	4.5
S51	53.4	37.4	4.3	2.1	26.3	71.7	84.6	0.6	0.3	1.0	0.0	33.8	1.5	11.2	15.9	6.7	20.4	0.5	0.0	4.0	2.2	2.5	0.0	0.0	0.0	19.9	64.2	15.9	3.4
MEAN	**47.3**	**38.7**	**8.6**	**8.6**	**67.0**	**24.4**	**89.1**	**0.3**	**2.1**	**7.4**	**4.5**	**35.0**	**1.7**	**14.7**	**14.0**	**6.5**	**7.9**	**1.1**	**0.4**	**1.3**	**2.3**	**1.0**	**0.1**	**0.0**	**0.0**	**39.3**	**47.7**	**13.1**	**5.0**
STDDEV	**9.9**	**8.3**	**5.8**	**8.9**	**19.6**	**20.3**	**4.9**	**0.1**	**1.8**	**5.1**	**3.1**	**7.9**	**2.7**	**4.0**	**3.7**	**2.3**	**6.6**	**0.8**	**0.4**	**1.4**	**1.4**	**1.0**	**0.1**	**0.0**	**0.1**	**15.9**	**14.0**	**4.6**	**1.3**

Sample	Depth	DML	DSOM	GRV	SAN	MUD	$CaCO_3$	TOC	COR	RDA	HAL	BFO	PFO	GPO	BIV	ECH	BRY	SER	BAL	SCA	SPO	OST	SIL	SID	ACR	Ps	Ph	Po	FI
[]	[m]	[km]	[km]	[%]	[%]	[%]	[%]	[%]	[wt%]	[wt%]	[wt%]	[wt%]	[wt%]	[wt%]	[wt%]	[wt%]	[wt%]	[wt%]	[wt%]	[wt%]	[wt%]	[wt%]	[wt%]	[wt%]	[wt%]	[%]	[%]	[%]	[]
F. IV	*Foramol grain-supported carbonate sediment*																												
S02	32.2	11.7	20.9	5.1	88.9	6.0	82.7	0.2	2.3	5.3	0.2	49.7	0.0	14.6	6.7	7.9	7.0	0.8	0.2	2.2	0.0	1.6	0.2	0.0	1.2	50.6	37.7	11.7	5.9
S03	36.6	21.2	11.0	2.4	91.8	5.8	74.9	0.2	0.6	1.0	1.8	66.8	1.3	10.1	7.1	2.2	3.0	0.2	0.2	0.3	0.3	0.7	4.2	0.0	0.0	57.9	32.9	9.2	6.5
S07	43.2	23.6	12.1	3.9	88.6	7.5	80.7	0.2	0.7	0.9	0.0	56.3	0.9	10.0	12.1	5.5	8.8	0.9	0.7	1.2	0.2	1.2	0.0	0.0	0.6	30.1	60.1	9.8	4.3
S10	32.8	11.5	25.2	5.4	71.0	23.7	85.6	0.4	2.5	0.7	0.4	47.7	0.0	18.0	14.3	9.6	3.3	0.5	0.5	0.6	0.0	2.0	0.0	0.0	0.0	19.8	59.3	21.0	3.4
S12	47.5	17.8	18.2	0.3	44.2	55.4	81.7	0.5	0.1	0.2	0.1	50.1	5.6	10.7	13.4	11.3	0.9	0.0	0.0	5.6	0.5	0.5	1.2	0.0	0.0	3.7	84.0	12.3	2.2
S13	44.9	21.6	14.1	2.3	88.5	9.2	76.3	0.2	0.6	2.5	0.3	51.6	1.2	14.3	11.9	6.9	7.4	0.0	0.0	0.8	0.0	1.2	0.0	1.3	0.0	35.7	58.6	5.7	4.8
S18	44.6	29.1	10.3	3.8	75.5	20.7	80.7	0.3	1.1	1.3	0.1	55.4	0.5	11.2	9.6	3.4	8.4	0.7	0.1	0.7	0.8	1.9	0.4	4.3	0.0	40.6	52.4	7.1	5.2
S22	33.8	24.8	23.6	4.7	79.2	16.1	67.6	0.2	3.2	0.6	0.0	58.6	0.0	12.7	10.4	4.1	3.5	0.0	0.0	0.7	0.0	1.3	0.1	4.5	0.6	31.9	50.6	17.5	4.4
S24	46.7	40.9	6.0	1.7	72.6	25.7	72.0	0.2	0.5	1.7	0.8	55.3	0.8	14.2	7.2	1.2	7.1	0.1	0.0	0.3	1.1	0.6	9.3	0.0	0.0	45.8	46.4	7.8	5.6
S34	42.0	27.0	14.3	1.4	45.6	53.0	83.2	0.5	0.3	0.4	0.0	53.7	1.2	10.1	17.6	6.7	3.0	0.0	0.0	5.3	0.0	1.7	0.0	0.0	0.0	23.3	55.3	21.3	3.7
S43	43.7	27.4	10.7	1.8	44.7	53.5	84.6	0.5	0.6	1.1	4.9	51.0	0.3	11.7	15.3	7.0	4.7	0.0	0.0	1.6	0.0	1.7	0.1	0.0	0.0	29.6	53.1	17.3	4.2
S44	46.9	35.0	3.8	4.4	85.8	9.8	95.8	0.2	1.0	4.1	6.3	61.0	0.0	9.4	5.3	5.1	3.8	1.1	0.0	0.0	2.7	0.2	0.0	0.0	0.0	64.1	26.3	9.6	7.0
MEAN	**41.2**	**24.3**	**14.2**	**3.1**	**73.0**	**23.9**	**80.5**	**0.3**	**1.1**	**1.6**	**1.2**	**54.8**	**1.0**	**12.2**	**10.9**	**5.9**	**5.1**	**0.4**	**0.1**	**1.6**	**0.5**	**1.2**	**1.3**	**0.8**	**0.2**	**36.1**	**51.4**	**12.5**	**4.8**
STDDEV	**5.8**	**8.6**	**6.7**	**1.6**	**18.3**	**19.4**	**7.2**	**0.1**	**1.0**	**1.6**	**2.1**	**5.4**	**1.5**	**2.6**	**3.9**	**2.9**	**2.6**	**0.4**	**0.2**	**1.9**	**0.8**	**0.6**	**2.8**	**1.7**	**0.4**	**16.9**	**14.9**	**5.4**	**1.4**
F. V	*Foramol mud-supported carbonate sediment*																												
S06	35.7	13.7	21.4	9.0	76.2	14.8	71.5	0.3	3.2	1.8	0.0	35.5	1.0	11.8	16.9	7.2	4.1	0.0	1.4	1.5	0.3	1.4	1.1	12.7	0.0	23.6	63.1	13.4	3.8
S09	34.7	7.0	30.4	7.0	51.1	41.8	70.0	0.6	0.3	0.0	0.0	36.4	0.0	12.8	28.2	14.5	3.3	0.1	0.7	1.7	0.0	2.0	0.0	0.0	0.0	11.9	69.0	19.0	2.8
S11	44.2	14.0	22.3	0.9	38.4	60.7	79.7	0.5	0.8	0.0	0.0	42.9	1.8	13.0	19.4	12.9	2.3	0.0	0.0	3.9	0.5	2.6	0.0	0.0	0.0	9.6	71.1	19.3	2.6
S16	34.3	13.1	30.3	8.9	53.2	37.9	75.4	0.5	1.2	0.0	0.0	36.1	0.0	17.2	31.6	9.6	0.4	0.0	0.0	1.1	0.0	1.7	0.2	0.0	0.9	9.8	71.2	19.0	2.6
S17	51.1	20.2	20.3	0.9	32.1	67.0	79.7	0.7	0.2	0.0	0.0	40.2	3.3	15.3	21.7	8.0	0.5	0.3	0.0	7.5	0.4	2.5	0.0	0.0	0.0	9.7	68.2	22.1	2.6
S21	27.9	16.5	32.0	6.1	65.1	28.7	77.3	0.4	1.2	0.2	0.3	41.8	0.0	12.5	28.9	10.3	1.2	0.0	0.1	1.6	0.9	0.6	0.6	0.0	0.0	19.1	57.3	23.6	3.3
S23	43.6	25.2	13.8	1.1	31.7	67.2	85.1	0.5	0.5	0.0	0.0	36.9	2.9	13.8	23.3	9.8	2.9	0.0	0.0	5.4	0.3	4.0	0.0	0.0	0.0	13.4	61.1	25.5	2.8
S26	23.1	16.9	35.7	5.7	81.7	12.6	69.5	0.2	0.5	1.2	0.6	50.1	0.0	11.9	18.7	9.4	0.7	0.0	0.0	0.4	0.6	0.8	3.5	0.3	1.4	22.0	62.7	15.3	3.6
S33	27.4	15.2	24.2	9.9	78.4	11.7	62.7	0.3	1.5	1.3	0.9	44.9	0.0	16.3	16.9	4.6	1.6	0.4	0.7	0.2	0.2	0.7	0.9	7.9	0.9	26.9	56.7	16.4	4.0
S42	39.0	18.3	20.3	10.5	55.8	33.7	81.2	0.8	0.0	0.0	0.0	42.7	0.7	15.3	34.1	2.8	2.7	0.0	0.0	1.1	0.2	0.4	0.0	0.0	0.0	23.8	59.6	16.6	3.7
S48	34.7	21.9	22.1	1.8	29.5	68.7	77.8	0.8	0.1	0.0	0.0	37.5	1.1	12.9	27.9	9.9	2.1	0.0	0.0	3.0	0.0	5.5	0.0	0.0	0.0	11.7	42.1	46.2	2.5
S50	55.4	35.2	4.2	1.0	27.1	71.9	85.6	0.6	0.0	0.5	0.0	38.2	4.5	15.1	17.3	5.5	5.6	0.1	0.1	6.8	2.6	3.7	0.0	0.0	0.0	11.2	73.7	15.1	2.7
MEAN	**37.6**	**18.1**	**23.1**	**5.2**	**51.7**	**43.1**	**76.3**	**0.5**	**0.8**	**0.4**	**0.2**	**40.3**	**1.3**	**14.0**	**23.7**	**8.7**	**2.3**	**0.1**	**0.3**	**2.8**	**0.5**	**2.2**	**0.5**	**1.7**	**0.3**	**20.6**	**59.1**	**20.3**	**3.4**
STDDEV	**9.6**	**7.1**	**8.6**	**3.9**	**20.2**	**23.3**	**6.8**	**0.2**	**0.9**	**0.6**	**0.3**	**4.4**	**1.5**	**1.8**	**6.1**	**3.3**	**1.6**	**0.1**	**0.4**	**2.5**	**0.7**	**1.6**	**1.0**	**4.1**	**0.5**	**15.7**	**13.0**	**9.5**	**1.3**
F. VI	*Mixed carbonate-siliciclastic sand*																												
S04	68.8	31.0	1.9	2.8	92.4	4.9	43.3	0.1	0.1	1.4	0.5	32.6	6.4	12.0	3.9	2.7	1.7	1.3	0.0	1.5	2.1	0.2	33.5	0.0	0.0	40.5	47.1	12.4	5.1

392

https://doi.org/10.5194/egusphere-2026-3460
Preprint. Discussion started: 5 August 2026

3.6 Integrated multivariate relationships

Principal component analysis (PCA) integrating foraminiferal assemblages, spatial parameters (e.g., distance to mainland), and sedimentological variables (grain size, CaCO3, TOC content) reveals a coherent cross-shelf gradient linking sediment-based facies and functional foraminiferal structure (Fig. 9A). Sample sedimentary facies (colour-coded) align along this gradient, with nearshore facies (I-II) clearly separated from mid- and outer shelf-facies, while partial overlap among facies III-V reflects transitional environmental conditions. Notably, the spatial distribution of samples with FI values in the marginal 2-4 range corresponds closely to the occurrence of facies V (foramol mud-supported carbonate sediment; Fig. 8A), providing independent convergent support for the intermediate ecological character of this transitional facies.

Stress-tolerant taxa show strong positive correlations with high mud content, elevated TOC, proximity to the mainland, and shallow water depth. Symbiont-bearing taxa, in contrast, show positive associations with sand-dominated substrates, high carbonate contents, and increasing distance from the mainland, as well as negative correlations with TOC and mud. Among these, *Operculina* exhibits particularly strong associations with greater water depth and high $CaCO_3$ content, compared to *Amphistegina*. Heterotrophic taxa occupy an intermediate position and display a lack of strong associations with either dominant grain size or spatial gradients, consistent with their broad distribution across mid- and nearshore settings.

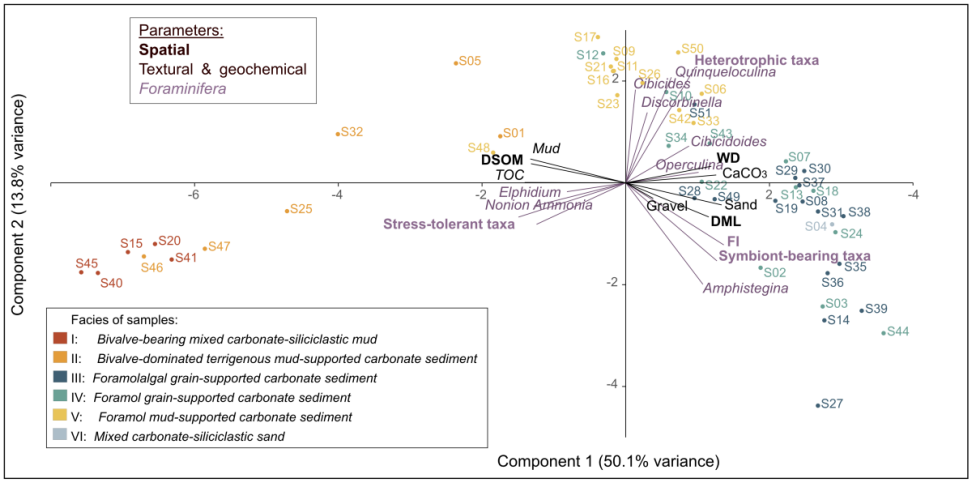

Figure 9. Integrated multivariate relationships of foraminiferal assemblages and sedimentary, and spatial parameters of inter-reef habitats of the Spermonde Archipelago. Principal Component Analysis (PCA) biplot integrating foraminiferal assemblages, FoRAM Index values (FI) and functional groups, spatial parameters, grain-size fractions, and geochemical variables. Samples are color-coded according to sedimentary facies. Component 1 explains 50.1% and Component 2 explains 13.8% of the total variance.

4 Discussion

The integrated sedimentological and foraminiferal datasets reveal strong along- and cross-shelf patterns with a particularly pronounced north–south asymmetry (Fig. 9, 10). As expected, nearshore environments are characterized by mud-rich, organic-enriched sediments and low FI values, whereas mid- to outer-shelf settings are

https://doi.org/10.5194/egusphere-2026-3460
Preprint. Discussion started: 5 August 2026

dominated by foramol facies and elevated abundances of symbiont-bearing larger benthic foraminifera (LBF). The cross-shelf profiles, in particular the different characteristics of the northern and the southern part, however, highlight that these transitions are not purely depth-controlled but reflect interactions among terrestrial input, seasonal forcing, and carbonate production. More broadly, these patterns challenge the classical dichotomy between photozoan and heterozoan carbonate systems, and instead support a continuum of mixed carbonate production modes on tropical shelves influenced by variable nutrient supply and light availability (Wilson & Vecsei 2005; Wilson, 2011; Mutti & Hallock, 2003). We therefore interpret the Spermonde shelf as a spatially structured system in which carbonate factory organization reflects shifting balances between autotrophic and heterotrophic components rather than discrete facies categories and discuss it in terms of threshold behaviour, organization, and seasonal modulation.

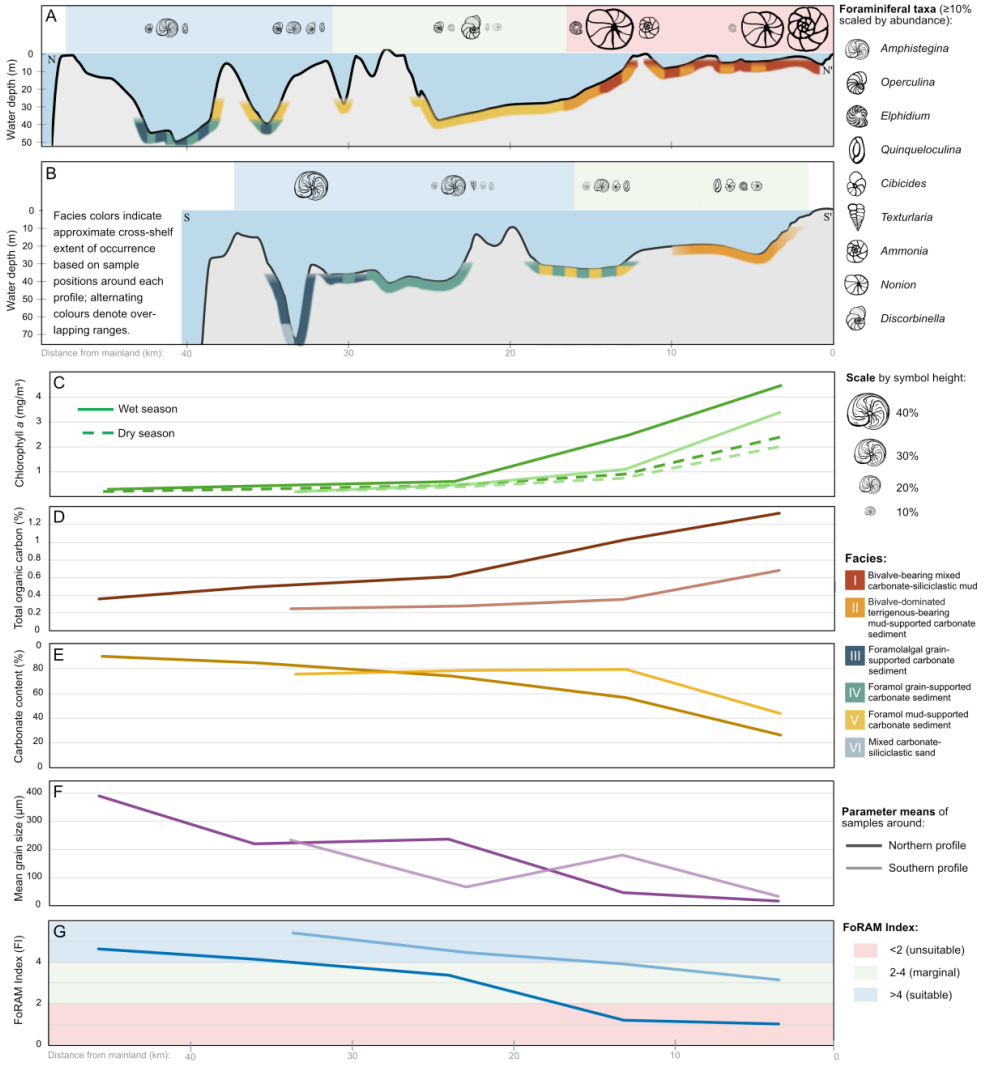

Figure 10. Cross-shelf synthesis profiles of the semi-enclosed Spermonde Archipelago indicating representative northern **(A)** and southern **(B)** shelf conditions (mean data of n ≥ 3 sampling station corridors extending north- and southwards from profile locations in Fig. 1). Facies colours along the seafloor profile indicate the approximate cross-shelf extent of each facies based

https://doi.org/10.5194/egusphere-2026-3460
Preprint. Discussion started: 5 August 2026

on sample positions around the respective profile; where two facies co-occur within the same distance range, colours alternate to indicate overlap. foraminiferal taxa with ≥10% relative abundance are shown as symbols scaled proportionally to abundance (see legend, with abundances between ~8 and 10% shown in grey). **(C)** Cross-shelf chlorophyll *a* concentrations during wet season (January) and dry season (August), derived from multiannual MODIS Aqua means (2003–2023; Fig. schematic representation based on satellite-derived spatial patterns, cf. Fig. 2E, F), **(D)** Total organic carbon (TOC) content (%), **(E)** calcium carbonate ($CaCO_3$) content (%), **(F)** mean grain size (µm), and **(G)** FoRAM Index (FI) values; each for the northern (dark lines) and southern (light lines) profiles. All panels shown from offshore (left) to nearshore (right); x-axes indicate distance from the respective mainland shoreline (km). Background shading in panels A, B and G indicate conditions suitable for reef growth (FI >4), marginal conditions (FI 2–4), and conditions unsuitable for reef growth (FI <2) following Hallock et al. (2003).

4.1 Threshold behaviour under terrestrial forcing

The nearshore shelf of the Spermonde Archipelago records a pronounced shift in sediment composition and carbonate-producing communities that can be better described as threshold behaviour than as a gradual cross-shelf transition, reflecting a non-linear response within the broader continuum of carbonate production modes rather than a departure from it. Facies I (bivalve-bearing mixed carbonate-siliciclastic mud) and facies II (bivalve-dominated terrigenous mud-supported carbonate sediment) are characterised by fine-grained, organic-enriched sediments, indicating the strong terrestrial input through fluvial discharge (Figs. 7-10). The tight statistical separation of these facies from all mid- and outer-shelf assemblages at the highest linkage distance in the cluster analysis (Fig. 7A) provides independent support for the interpretation that the compositional shift is discontinuous rather than gradual, consistent with a threshold response to terrestrial forcing rather than a progressive dilution of carbonate material along a trophic gradient.

Nearshore water clarity is chronically reduced across seasons, as indicated by persistently elevated chlorophyll concentrations (Fig. 2) and Secchi depths as low as 2.5 m during the wet season (Renema and Troelstra, 2001). This cross-shelf pattern in water clarity is corroborated by in-situ measurements along a cross-shelf transect, with chlorophyll *a* concentrations declining from 1.50 ± 0.21 µg L^{-1} in the nearshore zone to 0.14 ± 0.05 µg L^{-1} at the outer shelf (Kegler et al., 2017), a gradient consistent with the logarithmic decay documented over multiple years by Teichberg et al. (2018) and reflecting the non-linear attenuation of terrestrial influence with distance from the mainland. Under these conditions, skeletal assemblages are dominated by suspension- and filter-feeding taxa (notably bivalves) together with stress-tolerant benthic foraminifera and minor occurrences of echinoderms, ostracods and gastropods. Collectively, these represent a heterozoan association adapted to elevated nutrient loads and reduced light (Klicpera et al., 2014; Mutti and Hallock, 2003; Whatley, 1991). A comparable nutrient-driven dominance of heterotrophic carbonate producers has been documented from the Golfe d'Arguin under extensive upwelling and aeolian nutrient delivery (Klicpera et al., 2014), and along trophic gradients related to upwelling intensity in the Gulf of California, where increasing nutrient availability shifts assemblages to heterozoan dominance (Halfar et al., 2004). The Spermonde nearshore facies thus conform to broad nutrient-gradient models of carbonate factory organization, with fluvial discharge acting as a primary driver of trophic enrichment. In equatorial Southeast Asian shelf systems, such nutrient enrichment and associated turbidity are widely recognized as key controls on carbonate system organisation, compressing the euphotic zone and promoting the development of oligophotic carbonate platforms in which production occurs under persistently attenuated light conditions rather than within shallow, high-light reef environments (Wilson, 2012; Wilson and Vecsei, 2005).

The consistently low FI values in the nearshore-zone (<2 in the central and northern sectors) indicate conditions unfavourable for sustained photozoan carbonate production, in agreement with documented degradation pressures

https://doi.org/10.5194/egusphere-2026-3460
Preprint. Discussion started: 5 August 2026

on nearshore reef systems (Sari et al., 2021; Polónia et al., 2015) and with multiannual satellite evidence for increasing suspended sediment loads in this sector (Yasir Haya and Fujii, 2017), linked to extensive hinterland conversion (Cannon et al., 2007). The tight coupling between chlorophyll *a* concentrations and benthic community composition documented along the Spermonde cross-shelf transect (Kegler et al., 2017). supports the interpretation that the FI gradient recorded here reflects genuine environmental forcing rather than stochastic assemblage variation. Benthic foraminiferal assemblages are largely restricted to three stress-tolerant genera (*Nonion*, *Elphidium*, *Ammonia*), consistent with previous Spermonde studies (Girard et al., 2022; Renema, 2018; Renema and Troelstra, 2001) and with assemblages from other fluvially influenced settings such as the Gulf of California (Sánchez and Gómez-León, 2024) and the Persian Gulf (Saidova, 2010). The co-occurrence of elevated TOC, high mud content, and stress-tolerant assemblages support an interpretation of threshold-like habitat shifts rather than a simple carbonate dilution by terrigenous material.

The terrestrial influence is spatially asymmetrical. Facies II extends remarkably further offshore in the northern shelf sector (up to ~15 km; Table 3, Fig. 7B), implying disproportionate impacts of the Pangkajene and Segeri rivers relative to river systems on the central shelf. Given predominantly southward currents that follow the Makassar Strait circulation, this pattern is consistent with southward dispersal of river-derived material and nutrients (Gordon et al., 1999; Renema and Troelstra, 2001). Such along-shelf advection, combined with restricted cross-shelf flushing, likely enhances the persistence of turbid, nutrient-enriched conditions in the northern sector, thereby reinforcing the observed spatial threshold behaviour. In contrast, the southern nearshore zone records higher FI values (2.9-3.8; Fig. 8A) and increased proportions of symbiont-bearing (12-26%) and heterotrophic taxa (43-69%), suggesting comparatively improved photic conditions. Both the steeper FI rise and the narrower lateral extent of facies II in the southern cross-shelf profile (Fig. 10) are consistent with this interpretation, and align with the suggestion that dam construction in the Jene Berang catchment during the 1990s (Agnes et al., 2009), which reduced sediment discharge from the river, the largest fluvial input to the archipelago (Kneer, 2013), and may have partially mitigating terrestrial influence in the southern shelf sector (Hoeksema, 2012). Together, these observations indicate that relatively small differences in fluvial forcing and hydrodynamic retention can translate into disproportionate, threshold-like sedimentary and ecological responses – consistent with the sensitivity of rimmed shelf systems to catchment-scale changes, as suggested by comparison with more open platforms where such thresholds are absent (Burollet et al., 1986).

The semi-enclosed shelf setting, protected from open-marine currents and swells by its outer rim reefs, restricts exchange and promotes retention and lateral dispersal of fine sediments and associated nutrients (Figs. 1, 2, 10), consistent with spatial patterns of organic matter sources and hydrodynamic compartmentalisation previously documented for the archipelago (Rahayu et al., 2019). In nearshore sediment samples from nearshore settings, locally abundant authigenic gypsum crystals indicate reducing conditions associated with organic-rich, mud-dominated substrates (Schnitker et al., 1980), while the scarcity of balanids, serpulids, and bryozoans likely reflects limited availability of firm substrates in this low-energy, soft-bottom environment (Betzler et al., 1997; Umbgrove, 1928).

A marked regional contrast is provided by the Pater Noster Platform offshore SE Kalimantan (Borneo, Indonesia), which occupies a comparable climatic and bathymetric setting along the Makassar Strait (Burollet et al., 1986). Its seafloor sediments are sandy, supporting foramol and photozoan assemblages dominated by the symbiont-bearing foraminifera *Amphistegina*, *Operculina*, and *Calcarina*, as well as the calcifying macroalgae *Halimeda*, without the nearshore heterozoan threshold evident on the Spermonde shelf. Burollet et al. (1986) describe an incomplete

https://doi.org/10.5194/egusphere-2026-3460
Preprint. Discussion started: 5 August 2026

developed marginal reef barrier of the Pater Noster Platform. This difference may be attributed to the alongshore currents that redistribute fluvial discharge and limit sediment retention. In contrast, the rimmed architecture of the Spermonde shelf promotes fine-sediment retention, particularly in the northern sector, thereby amplifying nearshore heterozoan development. This comparison highlights that shelf architecture and hydrodynamic openness modulate the extent to which terrestrial forcing translates into threshold responses in carbonate factory organization.

An exception to the otherwise carbonate-dominated shelf is represented by facies VI (mixed carbonate-siliciclastic sand) on the outer southern shelf, interpreted as relict, potentially reflecting late Pleistocene deltaic or early Holocene transgressive deposits prior to full shelf flooding, comparable to seafloor sediment bodies described from the Sunda Shelf (Hanebuth et al., 2011). Minor occurrences of siliciclasts and siderites in mid-shelf samples (Fig. 6B, C; Table 2) may likewise represent reworked or relict components rather than active siliciclastic input.

4.2 Application of the FoRAM Index across inter-reef habitats

The strong spatial coherence between FI values and independently derived sedimentary facies validates the functional ecological signal beyond the shallow reef environments for which the FI was originally developed (Hallock et al., 2003). Most clearly expressed in the sharp contrast between nearshore FI <2 and the predominantly FI >4 mid-to-outer shelf (Fig. 8A), this correspondence confirms that the FI captures meaningful gradients in environmental suitability across the full cross-shelf transect, including the deeper inter-reef habitats (>50 m water depth). Notably, the FI 2-4 transitional zone in the central mid-shelf forms a spatially coherent north-south band that aligns closely with the distribution of facies V (foramol mud-supported carbonate sediment; Fig. 7B), providing independent evidence that both proxies record the same underlying environmental gradient. This agreement is particularly informative in equatorial mesotrophic settings, where sediment grain associations alone may not reliably differentiate between heterozoan- and photozoan-influenced production modes. The explanatory power of cross-shelf water quality gradients for benthic community composition in this system, with chlorophyll *a* alone accounting for a significant proportion of assemblage variance across an eight-station transect (Kegler et al., 2017), lends further support to the use of functional foraminiferal indices as integrative proxies for environmental conditions across inter-reef habitats. One interpretive caveat applies: FI values may overestimate photozoan suitability in mesotrophic settings where calcarinid taxa dominate under moderate nutrient enrichment (Minhat et al., 2024; Prazeres et al., 2020), though this bias is not expected to affect the inter-reef samples analysed here, which lack significant calcarinid contributions.

4.3 Benthic foraminifera as dominant carbonate producers

Beyond the nearshore threshold zone, the Spermonde shelf is characterized by the extensive development of foramol facies, which dominate most of the mid and outer-shelf (~80% of the investigated area; facies III-V). Across these settings, benthic foraminifers constitute the primary skeletal component and thus represent the dominant carbonate producers in the investigated inter-reef system. This prevalence of LBF is characteristic of oligophotic photozoan systems, in which carbonate production shifts to sediment-dominated factories composed of light-dependent but non-framework-building taxa. Such systems are widespread on equatorial shelves influenced by runoff or upwelling, where reduced light availability suppresses coral dominance but still permits substantial foraminiferal and coralline algal production (Wilson and Vecsei, 2005). On modern tropical shelves, larger benthic foraminifera may contribute substantially to reef-scale carbonate sediment production and can

https://doi.org/10.5194/egusphere-2026-3460
Preprint. Discussion started: 5 August 2026

locally rival or exceed contributions from corals and calcareous algae in inter-reef environments (e.g., Dawson and Smithers, 2014; Narayan et al., 2022), and their tests occur in a wide range of preservation states from pristine to heavily encrusted, indicating both active production and recycling within the sedimentary budget. In addition, LBF provide secondary hard substrates for epiphytic and encrusting biota such as bryozoans, further amplifying their functional role within the carbonate factory.

Within these foramol assemblages, the progressive offshore increase in symbiont-bearing taxa, particularly *Amphistegina* and *Operculina*, is consistent with greater light availability and oligotrophic conditions offshore favouring photozoan taxa, despite the persistence of mixed foramol grain associations. The occurrence of *Operculina* is strongly associated with greater water depth and high $CaCO_3$ contents, whereas *Amphistegina* occupies a broader depth range (Fig. 9, 10), consistent with previously documented species-level preferences across the Spermonde shelf (Renema, 2018; Renema et al., 2001). The broader ecological range of *Amphistegina* likely reflects the flexibility of its algal endosymbiont community, which is structured primarily by local environmental conditions rather than host species identity (Prazeres et al., 2021), underpinning its persistence across varying light and turbidity regimes. The preference of *Operculina* for deeper, lower-light environments is consistent with the morphological adaptation of flattened LBF facilitating efficient light capture under reduced irradiance (Hohenegger et al., 1999; Renema et al., 2001; Wilson, 2012), and supports an interpretation of increasing *Operculina* abundances offshore as reflecting not only depth trends but a progressive shift toward more stable, low-light carbonate production regimes.

Although the term “foramol” does not distinguish between photozoan and heterozoan contributors (an ambiguity previously noted for such assemblages; James, 1997; Kindler and Wilson, 2012; Lees, 1975; Lees and Buller, 1972) the co-occurrence of FI values and the relative abundance of symbiont-bearing taxa provides a functional discriminator that sediment composition alone cannot supply. This is most evident in the mid-shelf facies (facies IV and V), where heterotrophic taxa (e.g., *Quinqueloculina*, *Cibicidoides*, and *Cibicides*; Table S4) remain abundant alongside symbiont-bearing forms. Such foraminifera thrive in clear and turbid environments with low organic matter input (BadrElDin and Hallock, 2022; Lo Giudice Cappelli et al., 2019; Samir et al., 2003), and our PCA analyses confirm that they inhabit environments with sand-mud mixtures and medium TOC. The scatter of facies V samples across the transitional zone of the PCA biplot (Fig. 9A) reflects this mixed character: unlike the tightly clustered facies I-II samples, facies V occupies an intermediate position consistent with its role as a transitional assemblage between the nearshore heterozoan threshold and the more photozoan-influenced outer shelf. Such assemblages correspond to mixed heterozoan-photozoan associations *sensu* Mutti and Hallock (2003) and are consistent with the environmental ambiguity of equatorial carbonate systems, where humid tropical conditions support the simultaneous (co-)development of photozoan and heterozoan assemblages (Wilson, 2012). Only on the outer shelf does facies III approach a more classical photozoan configuration, with the highest relative proportions of red algae, *Halimeda* and coral (collectively ~14 wt%). These observations support a nuanced view of carbonate factory organisation on the Spermonde shelf in which a sharp nearshore threshold (driven by the retention of terrestrial input within the rimmed shelf architecture) gives way beyond the threshold zone to a continuum of mixed production modes in which photozoan contribution increases progressively offshore. Rather than contradicting one another, these two patterns operate at different points along the same environmental gradient, and their co-occurrence reflects the capacity of semi-enclosed tropical shelves to express both non-linear and gradational responses to terrestrial forcing. Resolving this structure requires integration of functional

https://doi.org/10.5194/egusphere-2026-3460
Preprint. Discussion started: 5 August 2026

ecological indicators with sedimentological facies analysis, since neither approach alone captures the full organisation of the carbonate factory.

4.4 Seasonal modulation of carbonate production

Monsoon seasonality acts as a fundamental driver of carbonate production across the Spermonde shelf, yet its effects are systematically spatially structured rather than uniform. During the northwest monsoon, enhanced precipitation and river discharge increase suspended particulate matter and nutrient delivery to the inner and mid shelf, temporarily reducing water transparency and elevating chlorophyll *a* concentrations (Nasir, 2016; Polónia et al., 2015; Teichberg et al., 2018). Satellite-derived SST and chlorophyll records confirm the steepening of nearshore–offshore gradients during peak wet-season discharge (Fig. 2), consistent with seasonal compression of the euphotic zone and temporary expansion of conditions unfavourable for symbiont-bearing carbonate producers. However, the spatial structure of these gradients, with chronically turbid nearshore waters and comparatively clear mid-to-outer shelf environments, persists across seasons, suggesting that monsoon forcing amplifies rather than creates the cross-shelf trophic gradient documented here.

This interpretation is supported by the limited interannual variability in benthic community composition relative to short-term water quality fluctuations (Girard et al., 2025; Renema and Troelstra, 2001; Teichberg et al., 2018), indicating that the assemblages recorded in the present sediment dataset reflect persistent environmental structuring rather than a seasonal snapshot. Elevated FI values on the mid and outer shelf are therefore interpreted as reflecting stable ecological conditions rather than transient dry-season intervals of high water-transparency. The capacity of *Amphistegina* and *Operculina* to adjust trophic strategies under reduced irradiance, facilitated by flexible symbiont associations and depth-partitioning (Hohenegger et al., 1999; Prazeres et al., 2021; Renema and Troelstra, 2001), further supports the persistence of photozoan-influenced carbonate production through seasonal turbidity pulses. The rimmed shelf morphology reinforces this stability: the outer rim and east-west trending channels restrict cross-shelf flushing during peak discharge events (Rahayu et al., 2019), promoting retention of terrigenous plumes in the nearshore zone and thereby limiting their seasonal penetration into mid- and outer-shelf environments.

Although upwelling influences reef communities along the outer rim (Hoeksema, 2012), the present inter-reef sediment data do not indicate a strong upwelling imprint on shelf-wide trophic gradients. The richest development of photozoan components on the outer shelf is more consistent with fluvial forcing as the primary cross-shelf control than with upwelling-driven nutrient enrichment. Long-term monitoring suggests that chronic land-based nutrient input may intensify rather than replace the natural seasonal signal (e.g., Natsir, 2022; Sari et al., 2021; Siringoringo et al., 2025), implying that ongoing coastal development in the Spermonde hinterland could shift the spatial threshold documented here progressively offshore, which warrants continued monitoring.

5 Conclusions

The Spermonde Archipelago illustrates how semi-enclosed tropical shelves respond non-linearly to terrestrial forcing under monsoon-dominated climatic regimes. Integrated sedimentological, geochemical, and foraminiferal datasets reveal a spatially structured carbonate factory in which nearshore environments, covering approximately 20% of the analysed area, undergo threshold-like shifts toward heterozoan-dominated assemblages under elevated fluvial nutrient input. The statistical separation of nearshore facies from all mid- and outer-shelf assemblages at

https://doi.org/10.5194/egusphere-2026-3460
Preprint. Discussion started: 5 August 2026

the highest cluster linkage distance, combined with consistently low FI values (<2) and stress-tolerant foraminiferal assemblages, supports an interpretation of discontinuous rather than gradual compositional change. This threshold is spatially asymmetrical: terrestrial influence extends disproportionately further offshore in the northern shelf sector, reflecting along-shelf advection of river-derived material under the prevailing Makassar Strait circulation, and contrasting with comparatively improved photic conditions on the southern shelf, where reduced fluvial input is consistent with catchment-scale modification of river discharge. This is most plausibly linked to impoundment of the Jene Berang River following dam construction in the 1990s (Hoeksema, 2012; Kneer, 2013) an intervention that may have measurably reduced the delivery of fine-grained terrigenous material to the southern shelf.

In contrast, the mid and outer shelf sustain extensive foramol production across approximately 80% of the investigated area, in which the proportion of photozoan components increases progressively offshore and carbonate production is driven largely by benthic foraminifera. These patterns demonstrate that carbonate production on the Spermonde shelf does not conform to a strict photozoan–heterozoan dichotomy, but instead reflects a continuum of mixed production modes structured by interacting gradients of terrestrial input, light availability, and hydrodynamic setting (Wilson and Vecsei, 2005).

The application of the FoRAM Index (FI, Hallock et al., 2003) demonstrates strong spatial coherence with independently derived sediment-based facies patterns, including a correspondence between the FI 2-4 transitional zone and the distribution of foramol mud-supported carbonate sediment facies, providing an independent ecological perspective on carbonate factory organisation. This agreement demonstrates that FI is particularly valuable in equatorial mesotrophic settings, where sediment component composition alone may not clearly differentiate between heterozoan- and photozoan-influenced carbonate production.

The rimmed shelf architecture enhances retention of fine-grained sediments and associated nutrients, amplifying cross-shelf contrasts and promoting threshold responses in nearshore habitats. Comparison with more open tropical platforms, where hydrodynamic exchange limits sediment retention and supports more uniformly photozoan assemblages (Burollet et al., 1986), underscores the critical role of platform geometry in modulating carbonate facies organisation. Monsoon seasonality amplifies rather than reorganises these spatial gradients, with seasonal turbidity pulses temporarily intensifying nearshore heterozoan conditions without fundamentally restructuring the shelf-wide carbonate factory. The persistence of stress-tolerant assemblages and chronically low FI values in the northern nearshore zone, in conjunction with documented increases in hinterland-derived suspended sediment loads over recent decades, suggests that ongoing coastal development may progressively shift the position of the threshold zone offshore, with implications for carbonate sediment budgets and reef condition across the archipelago.

Overall, the Spermonde Archipelago provides a modern example of how interactions among fluvial discharge, seasonal monsoon forcing, shelf-scale hydrodynamics, and ecological functional structure govern carbonate production in equatorial settings. These findings highlight that interpretations of tropical carbonate shelf systems benefit from combining sedimentological facies analysis with functional ecological indicators such as the FI, thereby expanding the interpretative framework for both modern and ancient carbonate systems.

https://doi.org/10.5194/egusphere-2026-3460
Preprint. Discussion started: 5 August 2026

Data availability

The data acquired and used for the present study are deposited in the PANGAEA data repository under identifier PDI-38754. The supplementary raw data tables for each sample are directly accessible under:

Table S1. Coordinates, water depth, carbonate and total organic carbon: https://doi.pangaea.de/10.1594/PANGAEA.994068

Table S2. Grain-size data from dry sieving and GRADISTAT analysis: https://doi.pangaea.de/10.1594/PANGAEA.994081

Table S3. Point-count data for skeletal and non-skeletal components: https://doi.pangaea.de/10.1594/PANGAEA.994082

Table S4. Benthic foraminiferal genus-level counts: https://doi.pangaea.de/10.1594/PANGAEA.994083

Appendix A – Additional Figures

Figure A1: Authigenic crystals from sample S45 (grain size fraction >2000 µm) identified as gypsum.

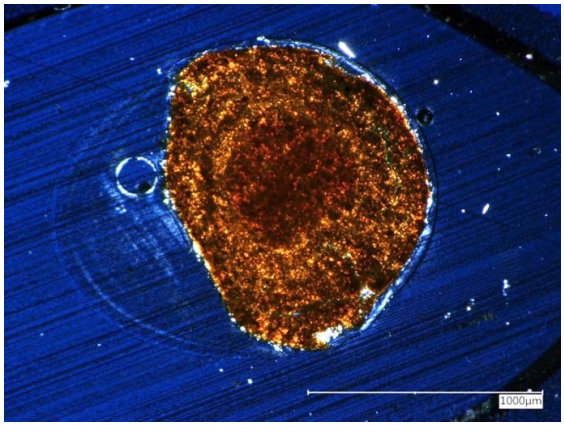

Figure A2. Thin-section of a siderite from sample S33 with concentric layering.

https://doi.org/10.5194/egusphere-2026-3460
Preprint. Discussion started: 5 August 2026

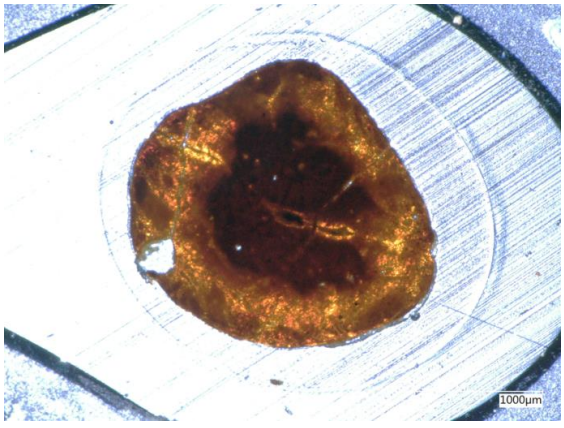

Figure A3. Thin-section of a siderite from sample S33 with larger dark nucleus and lighter outer layer(s).

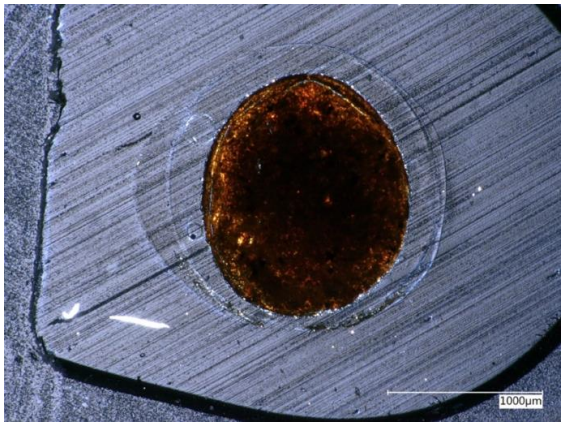

Figure A4. Thin section of a siderite from sample S33 with concentric layering close to the grain surface.

Author contributions

YK, TM and HW conceptualized the study. DK collected field samples and administered research permits. YK performed all lab analyses. YK performed original data analyses, prepared figures, and wrote the initial draft. MS curated data, performed formal analyses, and edited draft for submission. TM, MS, JJ and HW supervised research activities. TM secured the funding, MS, TM and HW administered the funding. All authors reviewed on the original draft.

Competing interests

The authors declare that they have no known competing financial interests or personal relationships that could have appeared to influence the work reported in this paper.

https://doi.org/10.5194/egusphere-2026-3460
Preprint. Discussion started: 5 August 2026

Disclaimer

Copernicus Publications remains neutral with regard to jurisdictional claims made in the text, published maps, institutional affiliations, or any other geographical representation in this paper. While Copernicus Publications makes every effort to include appropriate place names, the final responsibility lies with the authors. Views expressed in the text are those of the authors and do not necessarily reflect the views of the publisher.

Acknowledgements

This study is part of a cooperation between Hasanuddin University (UNHAS), Indonesia, and the Leibniz Centre for Tropical Marine Research (ZMT), Germany, and the research permit has been approved by the Ministry of Research and Technology of the Republic of Indonesia. Laboratory facilities were provided by the Leibniz Centre for Tropical Marine Research (ZMT). We thank Alessandro Reich, Ilham, Fidelia Moniz and Edi Kukang for their dedicated support during field work. We cordially would like to thank Sebastian Flotow for supporting the laboratory work.

Financial support

This research was funded through a grant from the Deutsche Forschungsgemeinschaft (DFG; grant no. MA6967/2-1) to TM in the SPP 1889 "Regional Sea Level and Society (SeaLevel)".

References

Agnes, R. D., Mochtar, S., Said, A., and Fujikura, R.: Effects of construction of the Bili-Bili Dam (Indonesia) on living conditions of former residents and their patterns of resettlement and return, International Journal of Water Resources Development, 25(3), 467–477, 2009.

BadrElDin, A. M. and Hallock, P. M.: Foraminifers associated with macroalgae on a wave-cut platform off Abu Qir coastal area, Egypt, Egyptian Journal of Aquatic Research, 48, 389–395, 2022.

Betzler, C., Brachert, T., and Nebelsick, J.: The warm temperate carbonate province a review of the facies, zonations, and delimitations, CFS Courier Forschungsinstitut Senckenberg, 201, 83–99, 1997.

Blott, S. J. and Pye, K.: GRADISTAT: A grain size distribution and statistics package for the analysis of unconsolidated sediments, Earth Surf Processes Landf, 26, 1237–1248, https://doi.org/10.1002/esp.261, 2001.

Brandano, M., Mateu-Vicens, G., and Baceta, J. I.: Understanding carbonate factories through palaeoecological and sedimentological signals – Tribute to Luis Pomar, Sedimentology, 69, 5–23, https://doi.org/10.1111/sed.12965, 2022.

Burollet, P. F., Boichard, R., Lambert, B., and Villain, J. M.: The Pater Noster carbonate platform, 155–169, 1986.

Cannon, C. H., Summers, M., Harting, J. R., and Kessler, P. J. A.: Developing conservation priorities based on forest type, condition, and threats in a poorly known ecoregion: Sulawesi, Indonesia, Biotropica, 39, 747–759, https://doi.org/10.1111/j.1744-7429.2007.00323.x, 2007.

Carannante, G., Esteban, M., Milliman, J. D., and Simone, L.: Carbonate lithofacies as paleolatitude indicators: Problems and limitations, Sedimentary Geology, 60, 333–346, https://doi.org/10.1016/0037-0738(88)90128-5, 1988.

Cleary, D. F. R., Becking, L. E., de Voogd, N. J., Renema, W., de Beer, M., Van Soest, R. W. M., and Hoeksema, B. W.: Variation in the diversity and composition of benthic taxa as a function of distance offshore, depth and

https://doi.org/10.5194/egusphere-2026-3460
Preprint. Discussion started: 5 August 2026

exposure in the Spermonde Archipelago, Indonesia, Estuarine, Coastal and Shelf Science, 65, 557–570, https://doi.org/10.1016/j.ecss.2005.06.025, 2005.

Dawson, J. L. and Smithers, S. G.: Carbonate sediment production, transport, and supply to a coral cay at Raine Reef, northern Great Barrier Reef, Australia: A facies approach, Journal of Sedimentary Research, 84, 1120–1138, https://doi.org/10.2110/jsr.2014.84, 2014.

Dunham, R. J.: Classification of Carbonate Rocks According to Depositional Texture, in: Classification of Carbonate Rocks – A Symposium, vol. 1, edited by: Ham, W. E., American Association of Petroleum Geologists, 0, 1962.

Estradivari, Pratama, A. M. A., Syafruddin, G., Kanna, P. L., Stuhr, M., Torres, A. F., Munawwarah, Ramos, D. A., Ambo-Rappe, R., Bejarano, S., Puebla, O., Wild, C., and Ferse, S. C. A.: Coastal urbanization-related stressors affect fish herbivory in the Spermonde Archipelago, Indonesia, Front. Mar. Sci., 12, 1359139, https://doi.org/10.3389/fmars.2025.1359139, 2025.

Flügel, E.: Methods, in: Microfacies of Carbonate Rocks: Analysis, Interpretation and Application, Springer Berlin Heidelberg, Berlin, Heidelberg, 53–72, https://doi.org/10.1007/978-3-662-08726-8_3, 2004.

Förderer, M., Rödder, D., and Langer, M. R.: Patterns of species richness and the center of diversity in modern Indo-Pacific larger foraminifera, Scientific Reports, 8, 8189, https://doi.org/10.1038/s41598-018-26598-9, 2018.

Girard, E. B., Estradivari, Ferse, S., Ambo-Rappe, R., Jompa, J., and Renema, W.: Dynamics of large benthic foraminiferal assemblages: A tool to foreshadow reef degradation?, Science of the Total Environment, 811, 151396, https://doi.org/10.1016/j.scitotenv.2021.151396, 2022.

Girard, E. B., Pratama, A. M. A., del Rio-Hortega, L., Volkenandt, S., Macher, J. N., and Renema, W.: Coastal eutrophication transforms shallow micro-benthic reef communities, Science of the Total Environment, 961, 178252, https://doi.org/10.1016/j.scitotenv.2024.178252, 2025.

Gonzales, M. B., Heyres, L. J., Monteclaro, H. M., del Norte-Campos, A. G., and Santander-de Leon, S. M. S.: Benthic foraminifera as bioindicator of coral reef condition in Nogas Island, Philippines, Regional Studies in Marine Science, 52, 102352, https://doi.org/10.1016/j.rsma.2022.102352, 2022.

Gordon, A. L., Susanto, R. D., and Field, A.: Throughflow within Makassar Strait, Geophysical Research Letters, 26, 3325–3328, https://doi.org/10.1029/1999GL002340, 1999.

Halfar, J., Godinez-Orta, L., Mutti, M., Valdez-Holguín, J. E., and Borges, J. M.: Nutrient and temperature controls on modern carbonate production: An example from the Gulf of California, Mexico, Geology, 32, 213, https://doi.org/10.1130/G20298.1, 2004.

Hallock, P.: The FoRAM Index revisited: Uses, challenges, and limitations, Proceedings of the 12th International Coral Reef Symposium, Cairns, Australia, July 9–13, 2012.

Hallock, P., Lidz, B. H., Cockey-Burkhard, E. M., and Donnelly, K. B.: Foraminifera as bioindicators in coral reef assessment and monitoring: The FORAM Index, in: Environmental Monitoring and Assessment, vol. 81, 221–238, 2003.

Hammer, Ø., Harper, D., and Ryan, P.: PAST: Paleontological statistics software package, 2001.

Hanebuth, T. J. J., Voris, H. K., Yokoyama, Y., Saito, Y., and Okuno, J.: Formation and fate of sedimentary depocentres on Southeast Asia's Sunda Shelf over the past sea-level cycle and biogeographic implications, Earth-Science Reviews, 104, 92–110, https://doi.org/10.1016/j.earscirev.2010.09.006, 2011.

Hoeksema, B. W.: Distribution patterns of mushroom corals (Scleractinia: Fungiidae) across the Spermonde shelf, South Sulawesi, The Raffles Bulleting of Zoology, 60(1): 183–212, 2012.

Hohenegger, J., Yordanova, E., Nakano, Y., and Tatzreiter, F.: Habitats of larger foraminifera on the upper reef slope of Sesoko Island, Okinawa, Japan, Marine Micropaleontology, 36, 109–168, 1999.

https://doi.org/10.5194/egusphere-2026-3460
Preprint. Discussion started: 5 August 2026

Ilahude, A. G.: On the occurrence of upwelling in the southern Makassar Strait, Marine Research in Indonesia, 10, 3–53, https://doi.org/10.14203/mri.v10i0.335, 1970.

James, N. P.: The cool-water carbonate depositional realm, in: Cool-Water Carbonates, vol. 56, edited by: James, N. P. and Clarke, J. A. D., SEPM Society for Sedimentary Geology, 0, https://doi.org/10.2110/pec.97.56.0001, 1997.

Janßen, A., Wizemann, A., Klicpera, A., Satari, D. Y., Westphal, H., and Mann, T.: Sediment composition and facies of coral reef islands in the Spermonde Archipelago, Indonesia, Frontiers in Marine Science, 4, 1–13, https://doi.org/10.3389/fmars.2017.00144, 2017.

Kegler, H. F., Lukman, M., Teichberg, M., Plass-Johnson, J., Hassenrück, C., Wild, C., and Gärdes, A.: Bacterial community composition and potential driving factors in different reef habitats of the Spermonde Archipelago, Indonesia, Front. Microbiol., 8, https://doi.org/10.3389/fmicb.2017.00662, 2017.

Kench, P. S. and Mann, T.: Reef island evolution and dynamics: Insights from the Indian and Pacific Oceans and perspectives for the Spermonde Archipelago, Front. Mar. Sci., 4, 145, https://doi.org/10.3389/fmars.2017.00145, 2017.

Kindler, P. and Wilson, M. E. J.: Carbonate grain associations: Their use and environmental significance, a brief review, in: Carbonate Systems during the Oligocene–Miocene Climatic Transition, John Wiley & Sons, Ltd, 35–47, https://doi.org/10.1002/9781118398364.ch3, 2012.

Klicpera, A., Michel, J., and Westphal, H.: Facies patterns of a tropical heterozoan carbonate platform under eutrophic conditions: The Banc d'Arguin, Mauritania, Facies, 61, 421, https://doi.org/10.1007/s10347-014-0421-5, 2014.

Kneer, D., Dynamics of seagrasses in a heterogeneous tropical reef ecosystem. PhD thesis, Christian-Albrechts-University Kiel, Germany, 2013.

Lees, A.: Possible influence of salinity and temperature on modern shelf carbonate sedimentation, Marine Geology, 19, 159–198, https://doi.org/10.1016/0025-3227(75)90067-5, 1975.

Lees, A. and Buller, A. T.: Modern temperate-water and warm-water shelf carbonate sediment contrasted, Marine Geology, 13, 1972.

Lo Giudice Cappelli, E., Clarke, J. L., Smeaton, C., Davidson, K., and Austin, W. E. N.: Organic-carbon-rich sediments: Benthic foraminifera as bio-indicators of depositional environments, Biogeosciences, 16, 4183–4199, https://doi.org/10.5194/bg-16-4183-2019, 2019.

Minhat, F. I., Safuan, C. D. M., Emran, S. A. M., Hasnizul, A. F. M., Afiq-Firdaus, A. M., Bachok, Z., and Talaat, W. I. A. W.: Uncovering foraminiferal assemblages in Pulau Redang and the importance of FoRAM index calibration for reef monitoring in South China sea, Marine Environmental Research, 202, 106825, https://doi.org/10.1016/j.marenvres.2024.106825, 2024.

Morgan, K. M., Moynihan, M. A., Sanwlani, N., and Switzer, A. D.: Light limitation and depth-variable sedimentation drives vertical reef compression on turbid coral reefs, Front. Mar. Sci., 7, https://doi.org/10.3389/fmars.2020.571256, 2020.

Müller, G. and Gastner, M.: The "Karbonat-bombe", a simple device for the determination of the carbonate content in sediments, soils and other materials, Neues Jahrb. Mineral., 10, 466–469, 1971.

Mutti, M. and Hallock, P.: Carbonate systems along nutrient and temperature gradients: Some sedimentological and geochemical constraints, International Journal of Earth Sciences, 92, 465–475, https://doi.org/10.1007/s00531-003-0350-y, 2003.

Narayan, G. R., Reymond, C. E., Stuhr, M., Doo, S., Schmidt, C., Mann, T., and Westphal, H.: Response of large benthic foraminifera to climate and local changes: Implications for future carbonate production, Sedimentology, 69, 121–161, https://doi.org/10.1111/sed.12858, 2022.

https://doi.org/10.5194/egusphere-2026-3460
Preprint. Discussion started: 5 August 2026

Nasir, A.: The use of C/N ratio in assessing the influence of land-based material in coastal water of South Sulawesi and Spermonde Archipelago, Indonesia, Front. Mar. Sci., https://doi.org/10.3389/fmars.2016.00266, 2016.

Natsir, S. M.: The distribution of benthic foraminifera in coral reefs ecosystem of East Penjaliran Island, Seribu Islands, Indonesia, Biodiversitas, 23, https://doi.org/10.13057/biodiv/d230634, 2022.

Neteler, M., Bowman, M. H., Landa, M., and Metz, M.: GRASS GIS: A multi-purpose open source GIS, Environmental Modelling & Software, 31, 124–130, https://doi.org/10.1016/j.envsoft.2011.11.014, 2012.

Sari N.W.P., Siringoringo, R. M., Abrar, M., Putra, R. D., Sutiadi, R. and Yusuf, S.: Status of coral reefs in the water of Spermonde, Makassar, South Sulawesi, E3S Web of Conferences, 324, https://doi.org/10.1051/e3sconf/202132403007, 2021.

Polónia, A. R. M., Cleary, D. F. R., de Voogd, N. J., Renema, W., Hoeksema, B. W., Martins, A., and Gomes, N. C. M.: Habitat and water quality variables as predictors of community composition in an Indonesian coral reef: A multi-taxon study in the Spermonde Archipelago, Science of the Total Environment, 537, 139–151, https://doi.org/10.1016/j.scitotenv.2015.07.102, 2015.

Prazeres, M., Martínez-Colón, M., and Hallock, P.: Foraminifera as bioindicators of water quality: The FoRAM Index revisited, Environmental Pollution, 257, https://doi.org/10.1016/j.envpol.2019.113612, 2020.

Prazeres, M., Roberts, T. E., Ramadhani, S. F., Doo, S. S., Schmidt, C., Stuhr, M., and Renema, W.: Diversity and flexibility of algal symbiont community in globally distributed larger benthic foraminifera of the genus *Amphistegina*, BMC Microbiology, 21, 1–16, https://doi.org/10.1186/s12866-021-02299-8, 2021.

Rahayu, Y. P., Solihuddin, T., Kusumaningtyas, M. A., Afi Ati, R. N., Salim, H. L., Rixen, T., and Hutahaean, A. A.: The sources of organic matter in seagrass sediments and their contribution to carbon stocks in the Spermonde Islands, Indonesia, Aquat Geochem, 25, 161–178, https://doi.org/10.1007/s10498-019-09358-7, 2019.

Rankey, E. C., Warrlich, G., Adams, E., Jakobsen, K. P., and Teoh, J.: Modern carbonate systems of Southeast Asia: Developing insights for understanding subsurface carbonate reservoirs in Southeast Asia, in: Cenozoic Isolated Carbonate Platforms – Focus Southeast Asia, vol. 114, edited by: Rankey, E. C. and Pöppelreiter, M. C., SEPM Society for Sedimentary Geology, 0, https://doi.org/10.2110/sepmsp.114.16, 2023.

Renema, W.: Terrestrial influence as a key driver of spatial variability in large benthic foraminiferal assemblage composition in the Central Indo-Pacific, Earth-Science Reviews, 177, 514–544, https://doi.org/10.1016/j.earscirev.2017.12.013, 2018.

Renema, W. and Troelstra, S. R.: Larger foraminifera distribution on a mesotrophic carbonate shelf in SW Sulawesi (Indonesia), Palaeogeography, Palaeoclimatology, Palaeoecology, 175, 125–146, https://doi.org/10.1016/S0031-0182(01)00389-3, 2001.

Renema, W., Hoeksema, B. W., and van Hinte, J. E.: Larger benthic foraminifera and their distribution patterns on the Spermonde shelf, South Sulawesi, Zool. Verh. Leiden, 334, 115–149, 2001.

Rosalina, D., Suryadi, L. P. F., Rombe, K. H., Leilani, A., Irwana, I., and Haris, R. B. K.: Salinity distribution pattern in Spermonde waters using remote sensing data (Copernicus Marine Service) in 2022, Jurnal Kelautan: Indonesian Journal of Marine Science and Technology, 17, 43–54, https://doi.org/10.21107/jk.v17i1.24098, 2024.

Saidova, Kh. M.: Benthic foraminifer communities of the Persian Gulf, Oceanology, 50, 61–66, https://doi.org/10.1134/S0001437010010078, 2010.

Samir, A. M., Abdou, H. F., Zazou, S. M., and El-Menhawey, W. H.: Cluster analysis of recent benthic foraminifera from the northwestern Mediterranean coast of Egypt, Revue de Micropaléontologie, 46, 111–130, https://doi.org/10.1016/S0035-1598(03)00018-7, 2003.

Sánchez, A. and Gómez-León, A.: Azoic sediments and benthic foraminifera: Environmental quality in a subtropical coastal lagoon in the gulf of California, Environmental Research, 244, 117924, https://doi.org/10.1016/j.envres.2023.117924, 2024.

https://doi.org/10.5194/egusphere-2026-3460
Preprint. Discussion started: 5 August 2026

Schnitker, D., Mayer, L. M., and Norton, S.: Loss of calcareous microfossils from sediments through gypsum formation, Marine Geology, 36, M35–M44, https://doi.org/10.1016/0025-3227(80)90085-7, 1980.

Sengupta, M., Mann, T., Stuhr, M., and Westphal, H.: Reef island morphological change over the past two decades: Spermonde Archipelago, Indonesia, Earth Surf Processes Landf, 50, e70152, https://doi.org/10.1002/esp.70152, 2025.

Siringoringo, R. M., Bengen, D. G., Nurjaya, I. W., Subhan, B., Giyanto, G., Putra, R. D., Abrar, M., Sari, N. W. P., and Aji, L. P.: Spatial variation in coral reef condition and reef fish assemblages along a proximity to Jakarta Bay, Indonesia, Biodiversitas, 26, https://doi.org/10.13057/biodiv/d261147, 2025.

Teichberg, M., Wild, C., Bednarz, V. N., Kegler, H. F., Lukman, M., Gärdes, A. A., Heiden, J. P., Weiand, L., Abu, N., Nasir, A., Miñarro, S., Ferse, S. C. A., Reuter, H., and Plass-Johnson, J. G.: Spatio-temporal patterns in coral reef communities of the Spermonde Archipelago, 2012–2014, I: Comprehensive Reef Monitoring of Water and Benthic Indicators Reflect Changes in Reef Health, Front. Mar. Sci., 5, 33, https://doi.org/10.3389/fmars.2018.00033, 2018.

Troelstra, S. R., Jonkers, H. M., and Rijk, D. S.: Larger foraminifera from the Spermonde Archipelago (Sulawesi, Indonesia), Scripta Geologica, 113, 93–120, 1996.

Umbgrove, J. H. F.: De koraalriffen van den Spermonde-Archipel (Zuid-Celebes), Leidse Geologische Mededelingen, 3, 228–247, 1928.

Veron, J. E. N., Devantier, L. M., Turak, E., Green, A. L., Kininmonth, S., Stafford-Smith, M., and Peterson, N.: Delineating the Coral Triangle, Galaxea, Journal of Coral Reef Studies, 11, 91–100, https://doi.org/10.3755/galaxea.11.91, 2009.

Ward, J. H.: Hierarchical grouping to optimize an objective function, Journal of the American Statistical Association, 58, 236–244, https://doi.org/10.1080/01621459.1963.10500845, 1963.

Wentworth, C. K.: A scale of grade and class terms for clastic sediments, The Journal of Geology, 30, 377–392, https://doi.org/10.1086/622910, 1922.

Westphal, H., Halfar, J., and Freiwald, A.: Heterozoan carbonates in subtropical to tropical settings in the present and past, International Journal of Earth Sciences, 99, 153–169, https://doi.org/10.1007/s00531-010-0563-9, 2010.

Whatley, R.: The platycopid signal: a means of detecting kenoxic events using Ostracoda, J. Micropalaeontol., 10, 181–185, https://doi.org/10.1144/jm.10.2.181, 1991.

Widagdo, S., Wibisono, D. V., and Prasita, V. D.: Upwelling Musiman di Perairan Spermonde, Sulawesi Selatan, 4, 2022.

Wilson, M. and Vecsei, A: The apparent paradox of abundant foramol facies in low latitudes: their environmental significance and effect on platform development, Earth-Science Reviews, 69, 133–168, https://doi.org/10.1016/j.earscirev.2004.08.003, 2005.

Wilson, M. E. J.: Cenozoic carbonates in Southeast Asia: Implications for equatorial carbonate development, Sedimentary Geology, 147, 295–428, https://doi.org/10.1016/S0037-0738(01)00228-7, 2002.

Wilson, M. E. J.: Equatorial carbonates: An earth systems approach, Sedimentology, 59, 1–31, https://doi.org/10.1111/j.1365-3091.2011.01293.x, 2012.

Wright, V. P. and Burgess, P. M.: The carbonate factory continuum, facies mosaics and microfacies: An appraisal of some of the key concepts underpinning carbonate sedimentology, Facies, 51, 17–23, https://doi.org/2010.1007/s10347-005-0049-6, 2005.

Yasir Haya, L. O. M. and Fujii, M.: Mapping the change of coral reefs using remote sensing and *in situ* measurements: A case study in Pangkajene and Kepulauan Regency, Spermonde Archipelago, Indonesia, Journal of Oceanography, 73, 623–645, https://doi.org/10.1007/s10872-017-0422-4, 2017.